AGU PUBLICATIONS

Paleoceanography

RESEARCH ARTICLE
10.1002/2014PA002674

Key Points:
- Deep-sea corals record rapid variability in the mid-depth NW Atlantic Ocean
- Centennial fluctuations of sourcing and radiocarbon during Heinrich Stadial 1
- Potential role for the intermediate ocean in early deglacial climate evolution

Supporting Information:
- Readme
- Table S1

Correspondence to:
D. J. Wilson,
david.wilson1@imperial.ac.uk

Citation:
Wilson, D. J., K. C. Crocket, T. van de Flierdt, L. F. Robinson, and J. F. Adkins (2014), Dynamic intermediate ocean circulation in the North Atlantic during Heinrich Stadial 1: A radiocarbon and neodymium isotope perspective, *Paleoceanography*, *29*, 1072–1093, doi:10.1002/2014PA002674.

Received 20 MAY 2014
Accepted 16 SEP 2014
Accepted article online 18 SEP 2014
Published online 20 NOV 2014

Dynamic intermediate ocean circulation in the North Atlantic during Heinrich Stadial 1: A radiocarbon and neodymium isotope perspective

David J. Wilson[1], Kirsty C. Crocket[1,2], Tina van de Flierdt[1], Laura F. Robinson[3,4], and Jess F. Adkins[5]

[1]Department of Earth Science and Engineering, Imperial College London, London, UK, [2]Scottish Association for Marine Science, Scottish Marine Institute, Oban, UK, [3]School of Earth Sciences, University of Bristol, Bristol, UK, [4]Department of Marine Chemistry and Geochemistry, Woods Hole Oceanographic Institution, Woods Hole, Massachusetts, USA, [5]Caltech Division of Geology and Planetary Sciences, MS 131-24, Pasadena, California, USA

Abstract The last deglaciation was characterized by a series of millennial-scale climate events that have been linked to deep ocean variability. While often implied in interpretations, few direct constraints exist on circulation changes at mid-depths. Here we provide new constraints on the variability of deglacial mid-depth circulation using combined radiocarbon and neodymium isotopes in 24 North Atlantic deep-sea corals. Their aragonite skeletons have been dated by uranium-series, providing absolute ages and the resolution to record centennial-scale changes, while transects spanning the lifetime of a single coral allow subcentennial tracer reconstruction. Our results reveal that rapid fluctuations of water mass sourcing and radiocarbon affected the mid-depth water column (1.7–2.5 km) on timescales of less than 100 years during the latter half of Heinrich Stadial 1. The neodymium isotopic variability (−14.5 to −11.0) ranges from the composition of the modern northern-sourced waters towards more radiogenic compositions, suggesting the presence of a greater southern-sourced component at some times. However, in detail, simple two-component mixing between well-ventilated northern-sourced and radiocarbon-depleted southern-sourced water masses cannot explain all our data. Instead, corals from ~15.0 ka and ~15.8 ka may record variability between southern-sourced intermediate waters and radiocarbon-depleted northern-sourced waters, unless there was a major shift in the neodymium isotopic composition of the northern end-member. In order to explain the rapid shift towards the most depleted radiocarbon values at ~15.4 ka, we suggest a different mixing scenario involving either radiocarbon-depleted deep water from the Greenland-Iceland-Norwegian Seas or a southern-sourced deep water mass. Since these mid-depth changes preceded the Bolling-Allerod warming and were apparently unaccompanied by changes in the deep Atlantic, they may indicate an important role for the intermediate ocean in the early deglacial climate evolution.

1. Introduction

During the last deglaciation there was a dramatic shift in atmospheric composition and global climate that was punctuated by millennial-scale climate changes [*Clark et al.*, 2012]. In the North Atlantic region there were particularly strong swings between cold states (Heinrich Stadial 1 and the Younger Dryas) and warm states (Bolling-Allerod) before the relatively stable Holocene climate was established [*Johnsen et al.*, 1992; *Dansgaard et al.*, 1993; *Grootes et al.*, 1993; *Severinghaus and Brook*, 1999]. While orbital forcing may have provided the ultimate control on glacial-interglacial cycles [*Imbrie et al.*, 1992], the mechanisms involved in deglaciation were complex and are still not yet fully understood. Changes in ocean circulation may have played an important role through their effects on nutrient distributions, biological productivity, carbon storage, and heat transport [*Broecker and Denton*, 1989; *Sarnthein and Tiedemann*, 1990; *Clark et al.*, 2002; *Robinson et al.*, 2005; *Broecker et al.*, 2010; *Sigman et al.*, 2010; *Burke and Robinson*, 2012].

The modern Atlantic Ocean is predominantly ventilated by North Atlantic Deep Water (NADW), with incursions of Antarctic Intermediate Water (AAIW) at ~1 km depth, and Antarctic Bottom Water (AABW) below ~4 km depth in the western South Atlantic. This relatively stable Atlantic meridional overturning circulation (AMOC) influences regional climate by northward heat transport in the Gulf Stream and North Atlantic Drift and impacts global climate through the export of relatively warm, salty, nutrient-poor deep waters to the global oceans. During the last glacial period, the Atlantic Ocean circulation structure was reorganized, with a shoaling of

NADW to its glacial equivalent Glacial North Atlantic Intermediate Water (GNAIW) and its replacement at depth by southern-sourced waters (akin to modern AABW) below ~2–2.5 km and extending into the North Atlantic [*Curry and Oppo*, 2005; *Marchitto and Broecker*, 2006; *Lynch-Stieglitz et al.*, 2007; *Yu et al.*, 2008; *Roberts et al.*, 2010]. The deglacial transition appears to have been characterized by multiple switches between glacial and Holocene-like circulation modes [e.g., *Zahn and Stuber*, 2002; *Skinner et al.*, 2003; *McManus et al.*, 2004; *Skinner and Shackleton*, 2004; *Roberts et al.*, 2010] and possibly also by incursions of AAIW into the North Atlantic [e.g., *Schroder-Ritzrau et al.*, 2003; *Rickaby and Elderfield*, 2005; *Robinson et al.*, 2005; *Pahnke et al.*, 2008; *Thornalley et al.*, 2011b; *Hendry et al.*, 2014]. However, distinguishing between northern- and southern-sourced water masses at intermediate depths can be challenging and the presence of AAIW in the deglacial North Atlantic remains a subject of debate [e.g., *Yu et al.*, 2008; *Tessin and Lund*, 2013].

Additional and complementary insights into ocean circulation changes during the deglaciation may be obtained using neodymium (Nd) isotopes as a water mass tracer [*Frank*, 2002; *Goldstein and Hemming*, 2003]. Neodymium is supplied to the surface ocean by continental weathering, riverine inputs, and dust dissolution, imprinting deep water masses with characteristic Nd isotopic signatures that reflect the continental geology (i.e., time-integrated Sm/Nd ratios) surrounding their source regions. These are reported as ε_{Nd} values, the deviation in parts per 10,000 from the present-day composition of the Chondritic Uniform Reservoir ($^{143}Nd/^{144}Nd = 0.512638$) [*Jacobsen and Wasserburg*, 1980; *Wasserburg et al.*, 1981]. The oceanic residence time of Nd is ~500 years [*Tachikawa et al.*, 2003; *Siddall et al.*, 2008], shorter than the mixing time of the deep ocean, reflecting its particle-reactive behavior. Whereas conservative tracers such as temperature, salinity, and oxygen isotopes are set only by the boundary conditions in the source regions of the deep waters, for Nd isotopes it appears that the continental margins also represent a boundary that is felt by deep water masses through particulate-seawater interaction, termed "boundary exchange" [*Lacan and Jeandel*, 2005a; *Arsouze et al.*, 2009]. However, this process remains poorly understood in terms of the mechanisms involved, its magnitude, and geographic variability. Reversible scavenging of Nd by settling particles also leads to non-conservative behavior for this tracer, although this process generally has a stronger impact on Nd concentrations than Nd isotopes [*Siddall et al.*, 2008].

Despite these complexities, Nd isotopes appear to behave quasi-conservatively in the modern western Atlantic Ocean away from the subpolar regions of deep water formation [*von Blanckenburg*, 1999; *Siddall et al.*, 2008; *Rempfer et al.*, 2011]. This behavior reflects the relatively short advective timescales in this basin, in contrast to the Pacific Ocean where sluggish deep circulation allows non-conservative boundary exchange and reversible scavenging processes to be more strongly expressed [*Siddall et al.*, 2008; *Rempfer et al.*, 2011]. The advective behavior, together with distinct Nd isotopic compositions for modern-day NADW (−12.5 to −14.5) [*Piepgras and Wasserburg*, 1987] and southern-sourced waters (−8 to −9) [*Stichel et al.*, 2012], suggests that Nd isotopes may provide valuable insights into the evolution of northern- versus southern-sourced water masses in the Atlantic Ocean through time. Reconstructions of past Nd isotopic compositions in the Atlantic Ocean have been based on a range of substrates in sediment cores [e.g., *Rutberg et al.*, 2000; *Gutjahr et al.*, 2008; *Roberts et al.*, 2010; *Piotrowski et al.*, 2012; *Huang et al.*, 2014] and recently also on deep-sea corals [e.g., *van de Flierdt et al.*, 2006; *Colin et al.*, 2010; *Copard et al.*, 2010].

In this study, we reconstruct deglacial changes in mid-depth northwest Atlantic Ocean circulation and ventilation using a suite of uranium-series dated deep-sea corals from water depths of 1.1–2.6 km on the New England Seamounts. These depths are influenced by NADW today, but may have been sensitive to mixing between northern- and southern-sourced deep waters during the deglaciation. Significant episodes of coral growth at the New England Seamounts during Heinrich Stadial 1 [*Thiagarajan et al.*, 2013] afford us a particularly good window into this climatically important period, and unprecedented temporal resolution compared to previous paleoceanographic studies [*Robinson et al.*, 2014]. Our new Nd isotope measurements provide evidence for a highly dynamic mid-depth ocean. By combining Nd isotopes with radiocarbon, we also explore models of mixing between northern- and southern-sourced water masses that were previously proposed to explain rapid fluctuations in radiocarbon [*Adkins et al.*, 1998; *Robinson et al.*, 2005]. Overall, we suggest that important changes in mid-depth circulation occurred towards the end of Heinrich Stadial 1, preceding the circulation changes affecting the whole ocean at the onset of the Bolling-Allerod warming.

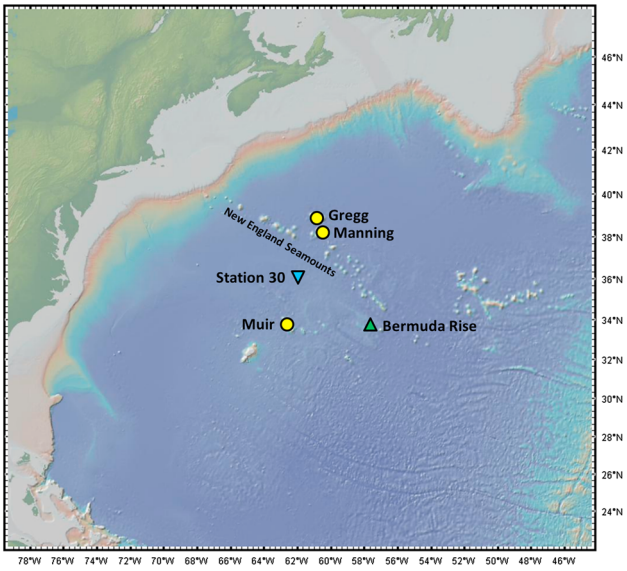

Figure 1. Location map for the New England Seamounts. Also shown is the location of the northwest Atlantic water column profile in Figure 2 (All 109-1 station 30 of *Piepgras and Wasserburg* [1987]) and the location of Bermuda Rise sediment core OCE326-GGC6 for which the Nd isotope record is shown in Figure 6 [*Roberts et al.*, 2010]. Base map from GeoMapApp.

2. Regional Setting and Samples

The studied deep-sea corals were collected from the New England Seamounts, a series of prominent bathymetric features in the northwest Atlantic Ocean at ~34–40°N (Figure 1). The modern-day oceanography in the region is dominated by Gulf Stream waters flowing north in the shallow layers and NADW flowing south in the deep western boundary current below ~1 km. The NADW bathing the New England Seamounts is not a homogeneous water mass, since Upper NADW (~1.0–2.2 km) contains a larger component of Labrador Sea Water, while the lower layers (Middle and Lower NADW; ~2.2–4.5 km) contain a larger component from the Greenland-Iceland-Norwegian Seas overflows, together with entrained open Atlantic waters [*Schmitz*, 1996]. The Nd isotopic signatures of these water masses are subtly different, with Upper NADW having a less radiogenic signature ($\varepsilon_{Nd} \sim -13.5$ to -14.5) than Middle and Lower NADW ($\varepsilon_{Nd} \sim -12.5$ to -13.5) (Figure 2) [see also *Lacan and Jeandel*, 2005b]. In comparison, southern-sourced waters in the Southern Ocean and South Atlantic have a more radiogenic Nd isotopic composition ($\varepsilon_{Nd} \sim -8$ to -9) (Figure 2). In the present day, those southern-sourced waters intrude into the South Atlantic above and below NADW as AAIW and AABW, respectively. Antarctic Intermediate Water can be traced into the equatorial Atlantic as a salinity minimum at ~0.5–1.2 km depth, with an ε_{Nd} value of approximately -10.5 reaching 8°N [*Huang et al.*, 2014], but neither AAIW nor AABW is present at the New England Seamounts today at the depths where we have corals.

Thousands of scleractinian corals were collected from the New England Seamounts by deep submergence vehicle *Alvin* and remotely operated vehicle *Hercules* during a series of cruises between 2003 and 2005 [*Robinson et al.*, 2007; *Thiagarajan et al.*, 2013]. Colonial corals (*Solenosmilia*, *Lophelia*, and *Enallopsammia*) were recovered from a depth range of 1.1–1.8 km, while solitary corals (mostly *Desmophyllum dianthus* but also some *Caryophyllia*) were recovered from depths of 1.1–2.6 km. Dating by uranium-series has indicated ages for the corals ranging from modern to over 200 ka, with a preference for growth during cold intervals and the majority of corals dating from the last glacial period [*Robinson et al.*, 2007].

In this study, a total of 24 solitary corals from Gregg, Manning, and Muir seamounts were selected for Nd isotope measurements. These corals cover an age range of 11–16 ka and a depth range of 1.1–2.6 km, although distributed unevenly (Figure 3). The majority of measurements were made on *D. dianthus*, with a few on *Caryophyllia*, both of which have been shown to record seawater Nd isotopes in a recent calibration [*van de Flierdt et al.*, 2010]. These samples were previously analyzed for uranium-series ages [*Adkins et al.*, 1998; *Adkins and Boyle*, 1999; *Robinson et al.*, 2005; *Eltgroth et al.*, 2006; *van de Flierdt et al.*, 2006; *Robinson et al.*, 2007] and many also for radiocarbon [*Adkins et al.*, 1998; *Adkins and Boyle*, 1999; *Robinson et al.*, 2005; *Eltgroth et al.*, 2006]. The original uranium-series ages from some of those studies [*Robinson et al.*, 2005; *Eltgroth et al.*, 2006; *van de Flierdt et al.*, 2006; *Robinson et al.*, 2007] have recently been updated (Robinson et al., Deep ocean radiocarbon constraints on carbon exchange during the last 30,000 years, manuscript in preparation, 2014), and we use those ages here, leading to a fully consistent uranium-series data set. The ability to date corals by uranium-series means that absolute and relatively precise dates can be obtained, with the benefit that radiocarbon can be used as an oceanographic tracer rather than a chronometer.

The corals were resampled for the Nd isotope measurements in this study (Table 1). Measurements were made on subsamples of 18 individual corals and each measurement likely integrates a period of less than

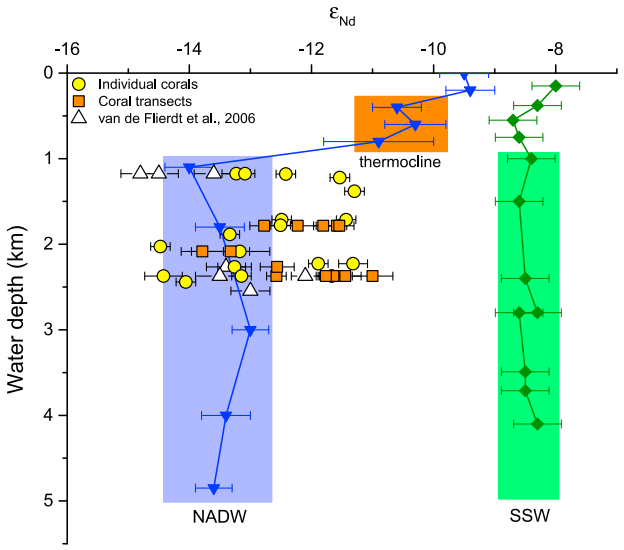

Figure 2. Modern water column Nd isotope profiles for the northwest Atlantic (blue triangles; All 109-1 station 30) [*Piepgras and Wasserburg*, 1987] and Southern Ocean (green diamonds; ANTXXIV/3 stations 113, 236, 241, 244) [*Stichel et al.*, 2012]. The blue, green, and orange bars highlight the approximate range of Nd isotopic compositions for NADW (−13.5 to −14.5 for Upper NADW and −12.5 to −13.5 for Middle and Lower NADW), southern-sourced waters (SSW; −8 to −9), and local thermocline waters (−10 to −11), respectively. The symbols show the Nd isotope data from deglacial deep-sea corals (11–16 ka). We distinguish transects from individual corals and also plot corals previously analyzed for Nd isotopes by *van de Flierdt et al.* [2006]. Uncertainties are shown as 2σ for both seawater and corals.

100 years, based on typical growth rates for deep-sea corals [*Adkins et al.*, 2004]. Six further corals were sampled as separate pieces along a transect parallel to the growth direction of the coral (typically top, middle, and bottom pieces) to correspond with previous transect sampling for radiocarbon measurements [*Adkins et al.*, 1998; *Eltgroth et al.*, 2006]. For such transect samples, the U-Th age reported for the bulk sample is applied to the top section of the transect, and the remaining ages are extrapolated using an age difference of 100 years between top and bottom pieces based on the growth rate estimates of *Adkins et al.* [2004]. This approach is imperfect, and we emphasize that these should not be taken to represent absolute ages for the individual sections, although the uncertainty in U-Th ages is typically larger than the lifespan of a coral. The value of the transect data is that stratigraphic direction is constrained, indicating the direction of change in the measured tracers through time, with the potential to record rapid changes in the ambient water column. The age uncertainty should be considered in interpreting the coral data set because two individual corals with the same reported age may have been growing at different times within their age uncertainties and could therefore record different tracer compositions if the water column experienced rapid changes. We emphasize this here as our results constitute the first attempt to constrain intermediate to deep water mass Nd isotope compositions on subcentennial timescales.

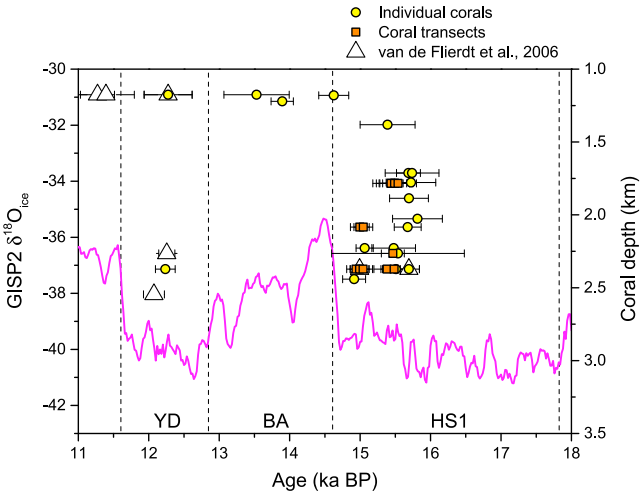

Figure 3. Depth-age plot of sampled deep-sea corals from the New England Seamounts. We distinguish transects from individual corals and also plot corals previously analyzed by *van de Flierdt et al.* [2006]. Also shown is the Greenland (GISP2) $\delta^{18}O_{ice}$ record [*Grootes et al.*, 1993; *Stuiver et al.*, 1995]. Age uncertainties on the corals are shown as 2σ. Stippled lines separate distinct time periods: YD = Younger Dryas, BA = Bolling-Allerod, and HS1 = Heinrich Stadial 1.

3. Methods

The coral cleaning, chemistry, and mass spectrometry are summarized here [after *van de Flierdt et al.*, 2010; *Crocket et al.*, 2014]. Coral cleaning is an important step because it removes potential sources of contamination from detrital particles or ferromanganese coatings that may be attached to fossil corals [*van de Flierdt et al.*, 2010]. The physical cleaning involved sand blasting and diamond blade drilling to remove ferromanganese coatings and detrital sediment from the exterior, and any interior cavities and discolored patches within the aragonite skeleton were cut

Table 1. Sample Details and Nd Isotope Data for Corals From the New England Seamounts[a]

Sample	Lab Code	Section	Site	Depth (m)	U/Th Age (yr BP)	2σ	^{14}C Age (yr BP)	2σ	ε_{Nd}	2σ	[Nd] (ng/g)
Individual Corals 1.7–2.5 km											
ALV-3887-1549-004-012	17	single	Muir	2372	12235	139	11340	70	−14.42	0.31	86
ALV-3887-1436-003-003	19	single	Muir	2441	14915	163	13585	70	−14.06	0.16	128
ALV-3884-1531-002-013	10	single	Muir	2228	15065	122	13840	60	−11.32	0.24	17
ALV-3884-1411-002-104	20	single	Muir	2228	15477	310	14145	60	−11.89	0.16	139
ALV-3887-1549-004-005	5	single	Muir	2372	15510	191	14015	60	−11.67	0.16	61
ALV-3887-1652-005-006-001	28	single	Muir	2265	15538	942	n.d.	n.d.	−13.26	0.27	48
ALV-3884-1638-004-014	6	single	Muir	2084	15675	191	14190	60	−13.17	0.16	60
ALV-3892-1315-001-B4-SS3	7	single	Manning	1713	15686	169	13840	60	−11.43	0.16	33
ALV-3887-1549-004-004	11	single	Muir	2372	15692	151	n.d.	n.d.	−13.15	0.16	35
ALV-3890-1330-002-007	18	single	Manning	1886	15694	275	14315	60	−13.34	0.16	78
ALV-3890-1407-003-003	8	single	Manning	1778	15722	352	13965	60	−12.50	0.16	116
ALV-3892-1315-001-003	13	single	Manning	1713	15738	381	14000	70	−12.49	0.16	65
ALV-3885-1239-001-012	3	single	Muir	2027	15814	354	14230	70	−14.47	0.16	109
Transect Corals 1.7–2.5 km											
ALV-3887-1549-004-002	44	top	Muir	2372	14943	133	13655	60	−11.00	0.33	85
ALV-3887-1549-004-002	44.2[b]	top	Muir	2372	14943	133	13655	60	−10.92	0.25	56
ALV-3887-1549-004-002	45	middle	Muir	2372	14993	133	13475	70	−12.57	0.16	81
ALV-3887-1549-004-002	46	bottom	Muir	2372	15043	133	13635	60	−11.64	0.25	109
ALV-3884-1638-004-210	41	top	Muir	2084	14996	133	13815	60	−13.79	0.35	41
ALV-3884-1638-004-210	42	middle	Muir	2084	15046	133	13602	56	−13.32	0.64	22
ALV-3887-1549-004-006	47	top	Muir	2372	15384	188	14315	70	−11.45	0.26	38
ALV-3887-1549-004-006	49	bottom	Muir	2372	15484	188	14275	70	−11.76	0.16	112
JFA 24.19	71	top	Manning	1784	15440	170	14500	100	−12.22	0.30	51
JFA 24.19	72	middle	Manning	1784	15490	170	14500	100	−12.77	0.24	33
JFA 24.8	74	top	Manning	1784	15440	260	14520	80	−11.58	0.16	36
JFA 24.8	75	middle	Manning	1784	15490	260	14470	100	−11.81	0.16	49
JFA 24.8	76	bottom	Manning	1784	15540	260	13850	80	−11.54	0.24	51
ALV-3887-1652-005-013	56	top	Muir	2265	15465	163	14375	60	−12.56	0.28	35
Individual Corals 1.1–1.4 km											
ALV-3891-1459-003-006-001 C	31	single	Gregg	1176	12275	341	n.d.	n.d.	−13.23	0.23	226
ALV-3891-1459-003-004	30	single	Gregg	1176	13530	463	12113	110	−13.09	0.16	346
ALV-3891-1758-006-007	15	single	Gregg	1221	13894	159	12470	60	−11.54	0.16	50
ALV-3891-1646-004-004	9	single	Gregg	1180	14626	212	12782	26	−12.42	0.16	118
ALV-3890-1742-007-001	4	single	Manning	1381	15390	390	13768	66	−11.30	0.16	126
Corals Contaminated for Authigenic Nd Isotopes[c]											
ALV-3887-1652-005-013	*58*	*bottom*	*Muir*	*2265*	*15565*	*163*	*14230*	*60*	*−14.08*	*0.29*	*193*
ALV-3885-1239-001-014	*14*	*single*	*Muir*	*2027*	*15791*	*183*	*14535*	*70*	*−14.32*	*0.16*	*264*
ALV-3889-1353-003-001	*12*	*single*	*Muir*	*1714*	*16436*	*822*	*14537*	*75*	*−13.99*	*0.16*	*772*
Corals From van de Flierdt et al. [2006]											
ALV-3891-1459-003-007	UAM05	single	Gregg	1176	11272	242	10286	120	−14.5	0.3	n.d.
ALV-3891-1459-003-006-002	UAM08	single	Gregg	1176	11392	404	n.d.	n.d.	−14.8	0.3	n.d.
ALV-3887-1324-002-002	UAI20	single	Muir	2546	12074	148	n.d.	n.d.	−13.0	0.3	n.d.
ALV-3887-1652-005-006-002	UAL12	single	Muir	2265	12256	114	n.d.	n.d.	−13.4	0.3	n.d.
ALV-3891-1459-003-006-001	UAM07[b]	single	Gregg	1176	12275	341	n.d.	n.d.	−13.6	0.3	n.d.
ALV-3887-1549-004-002	UAJ04[b]	single	Muir	2372	14993	133	n.d.	n.d.	−12.1	0.3	n.d.
ALV-3887-1549-004-004	UAK02[b]	single	Muir	2372	15692	151	n.d.	n.d.	−13.5	0.4	n.d.

[a]Lab codes correspond to *Crocket et al.* [2014] (numbers) or *van de Flierdt et al.* [2006] (combined letters and numbers). U-Th ages and ^{14}C ages are reported in years BP with 1950 as present (Robinson et al., manuscript in preparation, 2014); for details of original references see Table S1 in the supporting information. Nd isotope measurements are from this study, with data from *van de Flierdt et al.* [2006] also included. The 2σ reproducibility for Nd isotope measurements in this study represents the external reproducibility assessed from an in-house coral standard (0.16 ε_{Nd}). Where internal errors on an individual sample were larger than that external error, these errors were combined to give a total error from $\sqrt{\{(\text{internal error})^2 + (\text{external error})^2\}}$. Nd concentrations were measured by isotope dilution on TIMS, as described in *Crocket et al.* [2014]. n.d.: not determined.

[b]Identifies complete procedural replicates for Nd isotopes as described in the text.

[c]Data from corals considered contaminated for authigenic Nd isotopes (see text) are presented here for completeness and distinguished using italic font.

away. Subsequent sample preparation was performed in Class 10 laminar flow hoods in the MAGIC Clean Room Facility at Imperial College London (UK). Chemical cleaning was carried out in repeated oxidative and reductive steps, with final steps in ethylenediaminetetraacetic acid (EDTA) for the removal of adsorbed trace metals and leaching in dilute nitric acid (0.2%) for 1 min [*Cheng et al.*, 2000; *van de Flierdt et al.*, 2010]. Samples were then digested in 8 M HNO_3, dried down, and refluxed in aqua regia at high temperature (180–210°C). After conversion to nitrate, coral samples were taken up in a volume of 1.5 M HNO_3 sufficient to digest the carbonate plus 5% excess. After removing an aliquot for major and trace element analysis, the sample was spiked with ^{150}Nd and processed through chemistry.

Rare earth elements (REE) were separated from the carbonate matrix using Eichrom RE resin (100–150 μm bead size) in Teflon columns (resin bed volume of ~0.32 cm^3). Samples were loaded in 1.5 M HNO_3, the matrix was eluted in 4 mL 1.5 M HNO_3 and the REE fraction was collected in 4 mL 4 M HCl and dried at 120°C. Neodymium was isolated from the other REE using Eichrom Ln resin (20–50 μm bead size) in Teflon columns (resin bed volume of ~0.32 cm^3). Samples were loaded in 0.2 mL 0.142 M HCl, the light REE were eluted in 8.35 mL 0.142 M HCl, and the Nd fraction was collected in 3.5 mL 0.142 M HCl. After addition of 10 μL 0.001 M H_3PO_4, samples were dried at 120°C.

Neodymium isotopes were analyzed as Nd oxide by thermal ionization mass spectrometry (TIMS) on a ThermoFinnigan Triton in the MAGIC Laboratory at Imperial College London (UK), as described in *Crocket et al.* [2014]. Samples were loaded onto single tungsten filaments using a microsyringe, with TaF_5 activator and 2.5 M HCl. Filaments were preheated at 60 mA/min until 980°C, left for 30 min at this temperature, then further heated at 60 mA/min until ~1250°C, and the beam was subsequently tuned and peak centered multiple times before measurement at ~1500°C. Data were collected in nine blocks consisting of 20 integration cycles. Isobaric interferences from cerium and praseodymium oxides were corrected as described in detail in *Crocket et al.* [2014], and mass bias was accounted for using the exponential law and normalization to $^{146}Nd/^{144}Nd = 0.7219$. In each analytical session, five JNdi-1 standards were run on a turret, and the sample data were further corrected relative to the reference $^{143}Nd/^{144}Nd$ ratio of 0.512115 [*Tanaka et al.*, 2000]. Repeated measurements of the JNdi-1 standard (5 ng and 15 ng loads) over a period of 6 months yield $^{143}Nd/^{144}Nd = 0.512106 \pm 6$ (2σ), indicating a long-term reproducibility of 12 ppm or 0.12 ε_{Nd} units (2σ, $n = 44$). For an in-house coral standard (5, 10, and 30 ng loads), long-term reproducibility is 16 ppm or 0.16 ε_{Nd} units (2σ, $n = 13$), which is applied as the external reproducibility for sample measurements, or combined with internal errors where these are larger to give total uncertainties. Total procedural blanks, including coral digestion, column chemistry, and loading, were <5 pg ($n = 14$) and considered negligible.

The robustness of the cleaning procedure applied to these corals was considered in detail in *Crocket et al.* [2014], in which concentration measurements of Nd, Th, U, Fe, Mn, Ti, and Al of corals and external crusts removed from some of the corals were used to assess contamination from detrital sediments or ferromanganese crusts. That study suggested that three readily cleaned deglacial corals from the New England Seamounts could potentially be contaminated on the basis of elevated concentrations of these elements (Table 1) but otherwise demonstrated that the cleaning procedure applied was successful in removing contaminant phases. All the data discussed further are those that passed the screening of *Crocket et al.* [2014].

Three of the coral results reported here were also measured for Nd isotopes by *van de Flierdt et al.* [2006] and therefore provide complete procedural replicates from physical and chemical cleaning, through ion exchange chromatography to mass spectrometry by different methodologies in two different laboratories. Samples 11 (ALV-3887-1549-004-004) and 31 (ALV-3891-1459-003-006) were previously measured as individual corals, while transect samples 44/45/46 (ALV-3887-1549-004-002) correspond to a coral that was previously measured as an individual. In each case, the Nd isotopes are within error of the values reported by *van de Flierdt et al.* [2006] (Table 1). This good agreement also allows us to combine the new Nd isotope data set with four previously published measurements from early Holocene and Younger Dryas corals [*van de Flierdt et al.*, 2006].

4. Results

The Nd isotopic composition of seawater extracted from the aragonitic skeletons of deep-sea corals growing in 1.1–2.6 km water depth over the period 11–16 ka ranges from −11.0 to −14.8. This range not only

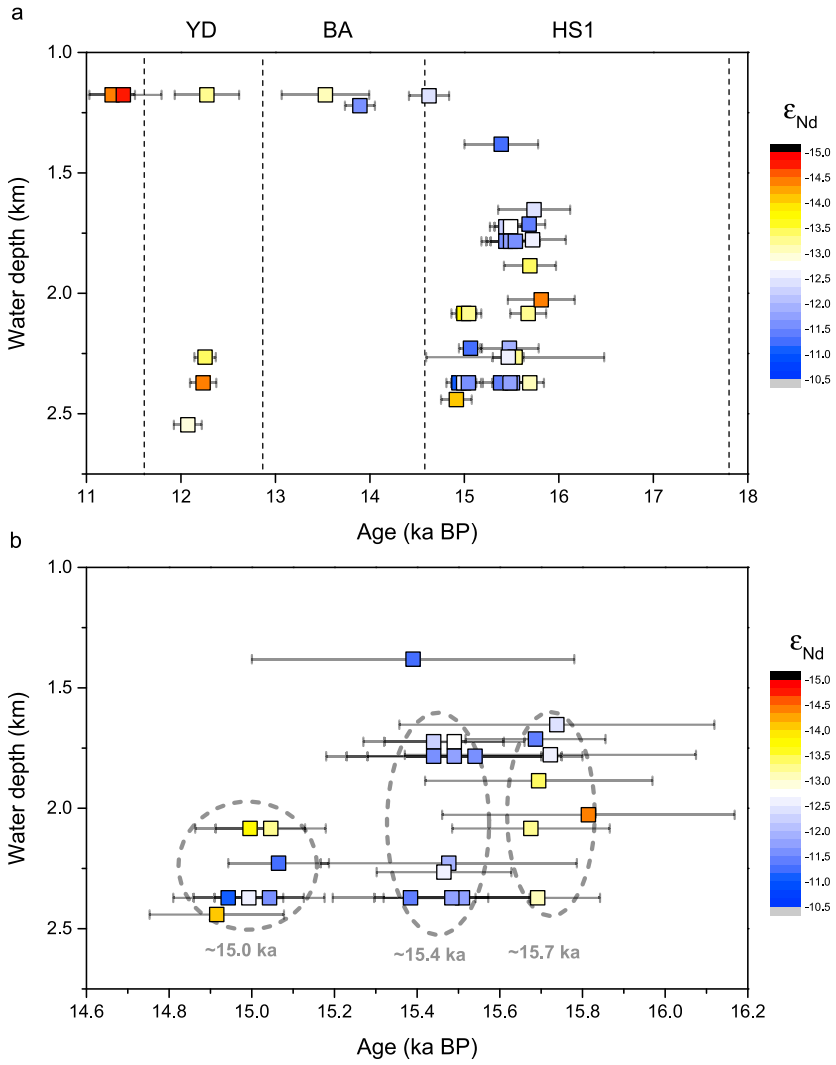

Figure 4. Deep-sea coral Nd isotopes versus depth and age for (a) 11–18 ka and (b) 14.6–16.2 ka. Neodymium isotope compositions are represented by color squares and 2σ age uncertainties are represented by horizontal grey bars. All data from both individual corals and transects are included, but coral ALV-3887-1652-005-006 is omitted from Figure 4b because of its large age uncertainty. Samples from JFA24.19 and ALV-3892-1315-001-003 are offset by 60 m on the depth axis to improve visualization. Stippled lines in Figure 4a separate distinct time periods: YD = Younger Dryas, BA = Bolling-Allerod, and HS1 = Heinrich Stadial 1. Ellipses in Figure 4b highlight three distinct periods of coral growth at the New England Seamounts during Heinrich Stadial 1.

encompasses the values of the modern water column in this location ($\varepsilon_{Nd} = -13$ to -14 between 1.1 and 3.0 km) [*Piepgras and Wasserburg*, 1987] but also extends to significantly more radiogenic values, with more than a third of all samples analyzed lying clearly outside the range defined by *Piepgras and Wasserburg* [1987] for modern NADW (blue bar in Figure 2).

Furthermore, there is very rapid temporal variability in Nd isotopic compositions on submillennial to centennial timescales. This variability is recorded in both the coral data set as a whole (Figures 4 and 5a) and in individual coral transects (Figure 5b). However, coral growth at the New England Seamounts was intermittent in time and depth and apparently mostly occurred during periods of climatic and oceanographic change [*Robinson et al.*, 2007; *Thiagarajan et al.*, 2013], such that the corals do not provide a complete record for all water depths at all times. Most of the corals analyzed are from Heinrich Stadial 1 (1.3–2.5 km depth) (Figure 4a) and these appear to fall within three distinct clusters at ~15.0 ka, ~15.4 ka, and ~15.7 ka (Figure 4b). Only two of the analyzed corals grew during the Bolling-Allerod warm period, and both are from ~1.2 km. A total of four samples date from the Younger Dryas, where samples from ~1.2 km and 2.3–2.5 km were analyzed.

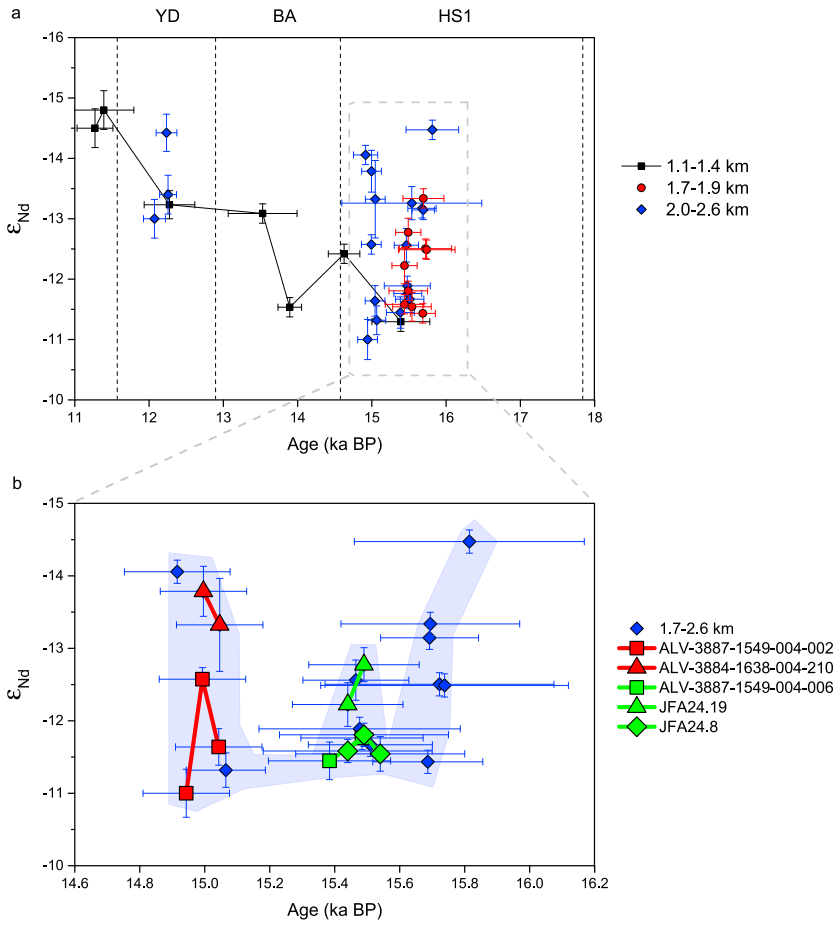

Figure 5. Deep-sea coral Nd isotope data as time series for (a) 11–18 ka and (b) 14.6–16.2 ka. Figure 5a distinguishes between depth ranges of 1.1–1.4 km, 1.7–1.9 km, and 2.0–2.6 km and includes all individual coral and transect data as single points. Figure 5b shows only data from depths of 1.7–2.6 km corresponding to the region highlighted by the grey box in Figure 5a. In Figure 5b the shaded blue field provides an indication of temporal changes in the data set as a whole, while the transect data are constrained stratigraphically and are distinguished with colored symbols and lines. All uncertainties are 2σ. Stippled lines in Figure 5a separate distinct time periods: YD = Younger Dryas, BA = Bolling-Allerod, and HS1 = Heinrich Stadial 1. Coral ALV-3887-1652-005-006 is omitted from Figure 5b because of its large age uncertainty.

To account for the uneven coral distribution through time, and more easily evaluate potential differences in Nd isotopes with water depth, the time series in Figure 5a distinguishes the seawater Nd isotope evolution over depth ranges of 1.1–1.4 km, 1.7–1.9 km, and 2.0–2.6 km. This division of the samples demonstrates that the two deeper depth ranges record similar ε_{Nd} values and evolution, and we subsequently consider the data from 1.7–2.6 km together (Figure 5b), but separately from the shallower corals (1.1–1.4 km).

During the deglacial period, seawater Nd isotopes from 1.7 to 2.6 km water depth vary between ε_{Nd} values of −11.0 and −14.5 (Figure 5a), and the evolution during the second half of Heinrich Stadial 1 is recorded in some detail (Figure 5b). There are unradiogenic values of −14.5 at ~15.8 ka, which increase towards −11.5 by ~15.6 ka. The corals record values of approximately −11.5 from ~15.5 ka to ~15.3 ka, with a transient fluctuation to −12.6 at ~15.4 ka. The third cluster at ~15.0 ka is characterized by a range in ε_{Nd} values from −11.0 to −14.1. Coral transect ALV-3887-1549-004-002 shifts towards −12.6 and then back to −11.0 at ~15.0 ka (Figure 5b), indicating that the changes towards a less radiogenic value at ~15.0 ka may have been a very transient feature lasting less than 100 years. Such short-lived changes represent a shorter time period than the typical 2σ uncertainty in coral U-Th ages, which could account for the high variability in Nd isotopes recorded at this time (Figures 4b and 5b). There are no corals from the 1.7–2.6 km depth range during the Bolling-Allerod, while three corals from this depth range within the Younger Dryas record Nd isotopic values in the range −13.0 to −14.4 (Figure 5a).

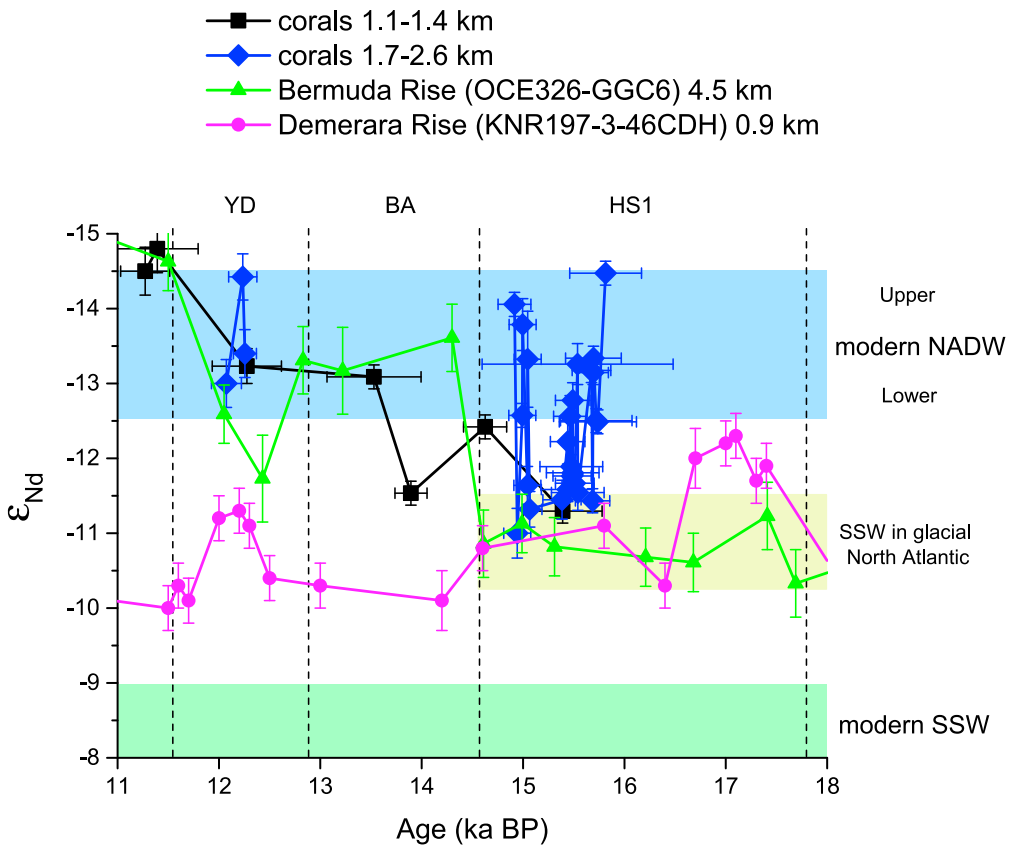

Figure 6. Deep-sea coral Nd isotope data compared to existing North Atlantic Nd isotope records over the period 11–18 ka. The deep Bermuda Rise record is from uncleaned foraminifera in core OCE326-GGC6 (~4.5 km) and is also supported by fish teeth data [*Roberts et al.*, 2010]. The intermediate depth Demerara Rise record is from uncleaned foraminifera in core KNR197-3-46CDH (~0.9 km) and is similar to Demerara Rise records from ~0.7 km and ~1.1 km depth [*Huang et al.*, 2014]. Both records are plotted on their published age models with 2σ error bars on ε_{Nd} values. Colored bars indicate the approximate compositions of modern NADW and southern-sourced waters (SSW) (see Figure 2) and the inferred composition of southern-sourced water in the glacial North Atlantic. Stippled lines indicate time periods: YD = Younger Dryas, BA = Bolling-Allerod, and HS1 = Heinrich Stadial 1.

There are relatively few data from the shallower depths (1.1 to 1.4 km), for which we have a lower resolution but more continuous record (Figures 4a and 5a). In general, we observe an increasingly unradiogenic ε_{Nd} composition through time, from −11.3 at 15.4 ka to −14.5 at 11.3 ka, with the exception of a reversal to −11.5 in one sample at ~13.9 ka within the Bolling-Allerod warm period. During both Heinrich Stadial 1 and the Younger Dryas, the Nd isotopic compositions of the shallower corals (ε_{Nd} values of −11.3 and −13.2, respectively) are within the range of the values recorded by the deeper corals at these times.

5. Discussion

5.1. Rapid Nd Isotope Variability at Mid-depths During Heinrich Stadial 1

The most striking aspect of our new data set is the rapidity of the changes recorded by Nd isotopes in the corals during Heinrich Stadial 1 (Figure 5b). For example, at ~15.0 ka there is variability between ε_{Nd} values of −11.0 and −14.0 within less than 200 years. Significant variability is also recorded within some transect samples (e.g., transect ALV-3887-1549-004-002; Figure 5b), which confirms that such rapid changes are a real feature of the data, rather than reflecting age uncertainties when comparing multiple corals. The transect data further indicate that some changes occurred in less than 100 years. Such extreme Nd isotope variability is not recorded in sediment core records over this time period, as demonstrated in Figure 6 where we make a comparison to records from the deep Bermuda Rise core OCE326-GGC6 (~4.5 km depth, see Figure 1 for location)

[*Roberts et al.*, 2010] and intermediate depth tropical Atlantic core KNR-197-3-46CDH (~0.9 km depth, 8°N, 54°W) [*Huang et al.*, 2014]. This discrepancy may indicate that sediment core records based on foraminiferal authigenic coatings do not have the ability to record such rapid changes in tracer composition; for example, due to pore water smoothing during signal acquisition, due to later bioturbation, or simply because of the lower sampling resolution. Therefore, we emphasize the unique value of the deep-sea coral archive for high-resolution studies. Alternatively, or in addition, the specific depth (~1.7–2.6 km) and time (late Heinrich Stadial 1) sampled by the corals at the New England Seamounts may have been particularly prone to rapid Nd isotope fluctuations. Here we explore the dynamic tracer behavior recorded in the corals at this time and place, while the question of how this variability compares to other archives and locations will require future research.

Rapid Nd isotopic changes occurring in less than 100 years may be explained by switching between different water masses, if those water masses carry distinct Nd isotope signatures and if there is a major front or water mass boundary nearby. We can describe this mechanism by reference to the modern-day water column in this location (Figure 2). There is a strong Nd isotope gradient at ~1 km depth, reflecting a front between the thermocline of the subtropical gyre overlying the Upper NADW. A small vertical shift in the position of that front by only ~200 m could produce a 3 ε_{Nd} shift in Nd isotopes; a similar magnitude to the changes recorded in the deglacial corals (Figure 5). If the thermocline was thicker during Heinrich Stadial 1 [e.g., *Hain et al.*, 2014] and shoaled towards its present thickness during the deglacial period, that could provide an explanation for the Nd isotope changes at 1.1–1.4 km depth (Figure 5a). Deglacial sea level changes of ~130 m [*Waelbroeck et al.*, 2002] could also contribute to this direction of change in Nd isotopes. In contrast, a mechanism involving thermocline changes does not seem reasonable to explain changes at depths of 1.7–2.6 km during Heinrich Stadial 1, which justifies treating the data from these two depth ranges separately. In the present contribution we focus mostly on the variability recorded at those deeper depths.

In the modern day, depths of 1.7–2.6 km at the New England Seamounts are occupied by Upper NADW and Middle NADW, although the boundary between these water masses is less distinct in Nd isotopes than the boundary to the thermocline above (Figure 2). Considering Heinrich Stadial 1, the water column structure may have differed quite significantly from the modern day. Indeed, the high variability in Nd isotopes over short timescales strongly suggests that the corals were growing close to a sharp gradient in Nd isotopes, indicating that this location was close to a hydrographic front at that time.

In addition to a vertical shift in frontal position, the Nd isotopic variability could also have been produced by a lateral shift in frontal position if the New England Seamounts were close to such a front during Heinrich Stadial 1. A better spatial resolution of deglacial Nd isotope data than exists at present within the North Atlantic basin would be required to distinguish between vertical or lateral frontal movements. However, in either case, our new data indicate a different oceanographic structure and greater variability in this region during Heinrich Stadial 1 in comparison to today. In the next section, we consider the constraints that the absolute Nd isotope values provide on those changes.

5.2. Neodymium Isotope Constraints on Water Mass Sources in the Deglacial Atlantic Ocean

In section 1 we highlighted the potential for Nd isotopes to distinguish between northern- and southern-sourced waters in the Atlantic Ocean, as demonstrated by the water column profiles in Figure 2 (i.e., northwest Atlantic versus Drake Passage). However, despite the strong link between Nd isotopes and Atlantic Ocean hydrography today [*von Blanckenburg*, 1999; *Siddall et al.*, 2008; *Rempfer et al.*, 2011], it is not possible to use Nd isotopes to provide quantitative constraints on past water mass mixing because the modern Atlantic hydrography is not a direct analogue for the glacial or deglacial Atlantic hydrography. First, uncertainties in the mechanism by which water mass Nd isotopic compositions and concentrations are set, together with the possibility of changing locations and/or modes of their formation in the past, combine to produce uncertainty in the expected Nd isotope end-members and mixing relationships in the past. Second, at times when the Atlantic Ocean was less well ventilated, such as during Heinrich Stadial 1 [*McManus et al.*, 2004], it was potentially more sensitive to non-conservative processes such as boundary exchange and reversible scavenging than it is today. An improved understanding of boundary exchange and particle scavenging in the modern Nd cycle is being addressed by the ongoing international GEOTRACES program which should improve future interpretations of paleoceanographic Nd isotope records. Here we outline the existing constraints on past end-member values, which is an empirical approach to that first question. For the southern-sourced waters

in particular, such an approach will likely always be necessary because that end-member is sensitive to the mixture of water masses supplying the intermediate and deep water formation zones and is therefore sensitive to the circulation itself. In order to fully address the second question, regarding possible non-conservative behavior, we would require a better spatial distribution of Nd isotope data throughout the glacial Atlantic basin to provide a more complete picture of Nd cycling in the past.

In the modern day, the Nd isotopic composition of NADW (Figure 2) is in the range of −13.5 to −14.5 in Upper NADW and −12.5 to −13.5 in Middle and Lower NADW [*Piepgras and Wasserburg*, 1987; *Lacan and Jeandel*, 2005b; *Lambelet et al.*, 2014]. However, changes in the proportions of deep water sourced from the Labrador Sea (−14.5) [*Lacan and Jeandel*, 2005b], Greenland-Iceland-Norwegian Seas overflows (−8 to −11) [*Lacan and Jeandel*, 2004b] and open ocean convection south of Iceland, or changes in the erosional inputs or boundary exchange in these regions [*von Blanckenburg and Nagler*, 2001; *Lacan and Jeandel*, 2005b], could have led to changes in the composition of NADW in the past. It has been suggested that over glacial-interglacial timescales, the composition of NADW/GNAIW in the northwest Atlantic was approximately constant using laser ablation data from ferromanganese crust BM1969.05 recovered from the San Pablo Seamount (39°N, 60°W, 1.8 km water depth) [*Foster et al.*, 2007]. However, these data do not rule out changes over shorter timescales. Existing data from deep-sea corals also suggested a rather constant NADW composition at the New England Seamounts [*van de Flierdt et al.*, 2006], although that study was based on a relatively small sample set that was discontinuous in time. In contrast, *Gutjahr et al.* [2008] suggested deglacial changes occurred in the NADW/GNAIW end-member based on sediment leachate data from the Blake Ridge, but the intermediate depth cores of that study appeared to be compromised by downslope sediment redistribution [*Gutjahr et al.*, 2008].

Since the modern water column in the northwest Atlantic Ocean samples the different northern end-members (i.e., Labrador Sea Water and Greenland-Iceland-Norwegian Seas overflow water) in different proportions at different water depths [*Lambelet et al.*, 2014], we suggest that Nd isotope variations in the range of −12.5 to −14.5 (blue bar in Figure 2) could be readily attributed to changes in those different contributions to NADW. Changes in the weathering inputs to those source regions could also generate values outside this range at times in the past; for example, highly unradiogenic Nd isotopic compositions could accompany elevated weathering in the Baffin Bay region [*von Blanckenburg and Nagler*, 2001]. In comparison to the modern day, the deglacial Nd isotope variations observed in the New England Seamount corals cover an even larger range from −11.0 to −14.5. Considering that this site is located downstream from the main deep water formation regions today and from proposed convection sites in the glacial North Atlantic Ocean [*Boyle and Keigwin*, 1987; *Labeyrie et al.*, 1992], this range of variability would either require more significant NADW end-member changes to have occurred or may be explained by contributions from southern-sourced waters.

In the South Atlantic Ocean, AAIW and AABW have relatively radiogenic Nd isotopic compositions of −8 to −9 in the modern day [*Jeandel*, 1993] (see also Figure 2). Therefore, mixing with either of these water masses could potentially generate the more radiogenic compositions of up to −11 recorded in the mid-depth corals (Figure 6). In order to constrain the past composition of southern-sourced waters, we focus here on Nd isotope measurements from deep-sea corals and uncleaned planktonic foraminifera, because in some cases these archives appear to provide more reliable evidence than reductive sediment leachates [*Elmore et al.*, 2011; *Kraft et al.*, 2013; *Wilson et al.*, 2013]. The existing evidence points towards a more radiogenic Nd isotopic composition of −6 to −7 for the deep Southern Ocean end-member during the last glacial period [*Robinson and van de Flierdt*, 2009; *Piotrowski et al.*, 2012], whereas Nd isotopes recorded from AAIW depths (~1 km) in the equatorial Atlantic were largely unchanged through the deglaciation at approximately −11 [*Huang et al.*, 2014] (Figure 6). The Nd isotopic composition of the deep glacial North Atlantic was also approximately −11 and has been interpreted as southern-sourced bottom water [*Roberts et al.*, 2010; *Gutjahr and Lippold*, 2011] (Figure 6). Since this value does not correspond to the composition of modern day or glacial deep Southern Ocean waters, it may indicate the admixture of some northern component into the southern-sourced waters along their northward flow path into the North Atlantic. Such a process is also observed today; for example, in the equatorial Atlantic the low-salinity signature of AAIW at ~1 km is accompanied by a Nd isotopic composition of approximately −10.5 [*Huang et al.*, 2014] that has evolved by mixing from its more radiogenic composition in the Southern Ocean. Therefore, we describe this end-member as southern-sourced water in the glacial North Atlantic Ocean (Figure 6).

In summary, deep-sea coral Nd isotope values in the range of −13.5 to −14.5 can be linked to the characteristic signature of modern-day Upper NADW (containing an unradiogenic Labrador Sea Water component), while values of −11 appear to correspond to the composition of southern-sourced waters in the glacial North Atlantic. Where intermediate values of approximately −12.5 are recorded, this signature could be the result of mixing between such northern- and southern-sourced water masses, or it may be linked to the composition of Middle NADW (i.e., a northern-source that is lacking the characteristically unradiogenic Labrador Sea Water signature), and we emphasize that it is not possible to distinguish between these possibilities from Nd isotopes alone. In addition, that second possible explanation highlights the ongoing challenge to constrain in detail the potential for changes through time in the Nd isotopic compositions of water mass end-members or their contributions to NADW in the open Atlantic Ocean.

5.3. Deglacial Variability of the Northwest Atlantic Water Column Structure

The Nd isotopic composition of −14.5 recorded at the New England Seamounts during the early Holocene (~11.5 ka) shows that there was no Nd isotope gradient between the intermediate ocean (this study) and the deep ocean [*Roberts et al.*, 2010] (Figure 6), consistent with the presence of NADW throughout the northwest Atlantic water column. In contrast, the deglacial corals record Nd isotope variability in the mid-depth ocean that provides evidence of significant and rapid (<100 years) changes in water mass structure during the latter half of Heinrich Stadial 1.

At ~15.8 ka, ~1 kyr after the onset of Heinrich event 1 [*Hemming*, 2004], there is a strong Nd isotope gradient between the mid-depth (this study) and deep [*Roberts et al.*, 2010] northwest Atlantic Ocean (Figure 6). Neodymium isotopes at mid-depths (approximately −13 to −14.5) are indicative of NADW/GNAIW while the deep ocean (approximately −10.5) is characterized by a large southern-sourced component. From 15.8 ka to 15.6 ka, seawater Nd isotopic compositions at 1.7–2.6 km water depth increase towards ε_{Nd} ~ −11.5 and almost converge with the contemporaneous deep northwest Atlantic ε_{Nd} value of approximately −11 (Figure 6), suggesting a dominant southern-sourced water contribution at mid-depths, which was mostly the case until ~15.1 ka. In contrast to the situation at ~15.8 ka, the lack of a Nd isotope gradient between mid-depth waters and the deep northwest Atlantic is consistent with a circulation mode in which the water column is dominantly southern-sourced with weakened and/or shoaled NADW/GNAIW overturning. However, over this period, there are also transient fluctuations to −12.6 at ~15.4 ka and to −14.1 at ~15.0 ka, which may suggest a return to a greater NADW/GNAIW influence at mid-depths at times when southern-sourced waters still dominated the deep northwest Atlantic (Figure 6).

Although our data do not constrain the water column structure during the peak ice rafting of Heinrich event 1, our evidence from the latter half of Heinrich Stadial 1 suggests a high degree of variability in water mass sourcing at mid-depths over this time, in contrast to unchanging water mass sourcing in the deep Atlantic Ocean throughout Heinrich Stadial 1 [*Roberts et al.*, 2010]. Such variability was also not observed in sedimentary $^{231}Pa/^{230}Th$ records from the deep Bermuda Rise, where $^{231}Pa/^{230}Th$ values were around the production ratio for the full duration of Heinrich Stadial 1 [*McManus et al.*, 2004] and may indicate continuously weakened deep-ocean overturning. However, the interpretation of $^{231}Pa/^{230}Th$ records in terms of circulation changes is not straightforward [*Burke et al.*, 2011; *Hayes et al.*, 2014], being influenced by the overlying water column [*Thomas et al.*, 2006] and by factors such as particle rain rate and composition [*Chase et al.*, 2002]. From our evidence on water mass sourcing, we conclude that the effect of Heinrich event 1 on the ocean circulation and structure was perhaps more complex than the view previously obtained from deep ocean records. In particular, our evidence points towards a highly dynamic mid-depth circulation in the North Atlantic during Heinrich Stadial 1, with the presence of southern-sourced waters but, at least episodically, also NADW/GNAIW contributions at mid-depths.

The deep northwest Atlantic Ocean records a major shift from −10.8 to −13.5 at the onset of the Bolling-Allerod (Figure 6), which was interpreted as a switch from southern-sourced waters to NADW [*Roberts et al.*, 2010]. One intermediate depth (1.2 km) coral (ε_{Nd} ~ −13.1) is consistent with the deep ocean value during the Bolling-Allerod, and a NADW/GNAIW dominance, whereas the other is significantly more radiogenic (ε_{Nd} ~ −11.5) (Figure 6). Neodymium isotopic variability at ~1.2 km depth could reflect variability between GNAIW and AAIW in the intermediate depth North Atlantic. Interestingly, the early Bolling-Allerod has been described as a period of intensified and/or deepened AMOC [*Barker et al.*, 2010], such that a denser, stronger,

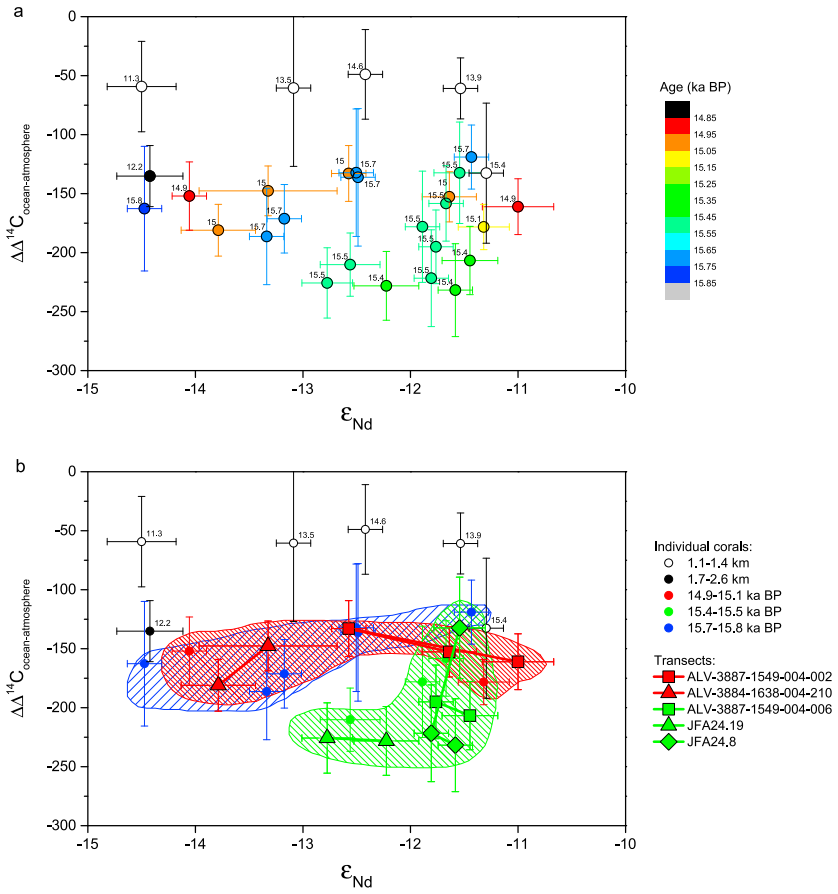

Figure 7. Radiocarbon ($\Delta\Delta^{14}C_{ocean-atmosphere}$) versus Nd isotope crossplots for the New England Seamounts. Figure 7a includes all deep-sea coral data from the New England Seamounts, with unfilled circles for the shallower depths (1.1–1.4 km), and filled circles for the deeper depths (1.7–2.6 km), which are color coded according to time intervals over the period 14.9–15.8 ka. Numbers next to symbols are ages in kiloannum BP. Figure 7b groups the deep data into three time periods over 14.9–15.8 ka (colored symbols and regions) and further distinguishes transect data with distinct symbols and connecting lines. All error bars are 2σ. Coral ALV-3887-1652-005-006 is omitted because of its large age uncertainty.

and deeper core of NADW/GNAIW may have been overlain by a northward-expanded AAIW at these shallower depths [*Came et al.*, 2008; *Huang et al.*, 2014]. Alternatively, the changes at ~1.2 km depth could reflect changes in thermocline thickness [*Hain et al.*, 2014], and more data from this interval are clearly required to better constrain the nature of these hydrographic changes.

During the Younger Dryas, ε_{Nd} values of −13.0 to −14.4 over the depth range of 1.1–2.6 km are consistent with the continued presence of NADW/GNAIW at intermediate and mid-depths, while the deep northwest Atlantic records a return towards a greater southern-sourced water component (ε_{Nd} ~ −11.7) (Figure 6). Therefore, whereas we demonstrate variability between northern- and southern-sourced waters at mid-depths during Heinrich Stadial 1, the Younger Dryas appears to represent a different scenario with less extreme changes in ocean circulation and a more Holocene-like mid-depth circulation regime.

5.4. Neodymium Isotope Evidence on Mid-depth Radiocarbon Evolution

In the modern ocean, NADW has an offset to atmospheric radiocarbon ($\Delta\Delta^{14}C = \Delta^{14}C_{ocean} - \Delta^{14}C_{atmosphere}$) of approximately −70‰, whereas southern-sourced waters have a larger offset of approximately −120‰ for AAIW and −165‰ for AABW [*Stuiver and Ostlund*, 1980] due to their differing formation mechanisms and longer storage time in the deep ocean. During the Last Glacial Maximum, poorer ventilation and longer storage times may have produced larger offsets of up to −300‰ or greater for southern-sourced waters [*Robinson and van de Flierdt*, 2009; *Barker et al.*, 2010; *Skinner et al.*, 2010; *Burke and Robinson*, 2012]. Fluctuations in radiocarbon in the North Atlantic during the deglacial period have therefore been interpreted

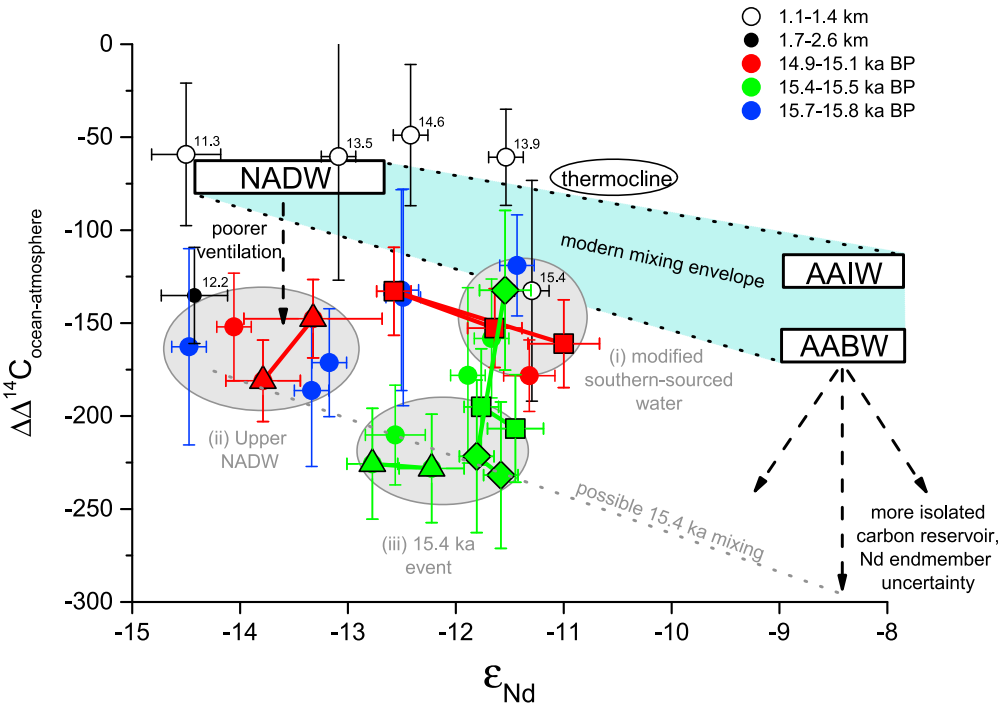

Figure 8. Radiocarbon ($\Delta\Delta^{14}C_{ocean\text{-}atmosphere}$) versus Nd isotope crossplot exploring potential end-members and mixing relationships for Heinrich Stadial 1 compared to the modern day. The values of NADW, AAIW, and AABW are modern values as described in the text, whereas the dashed arrows indicate possible shifts in these end-members during the late glacial period/Heinrich Stadial 1. The composition of the modern thermocline from Figure 2 is also shown. The grey ovals highlight the three regions (i), (ii), and (iii) described in the text and interpreted as follows: (i) modified southern-sourced water in the glacial North Atlantic; (ii) radiocarbon-depleted northern-sourced water (Upper NADW); and (iii) 15.4 ka event (either a Greenland-Iceland-Norwegian Seas source or mixing towards a radiocarbon-depleted deep southern-sourced water mass). Symbols are as in Figure 7b and numbers next to symbols are ages in kiloannum BP. The mixing lines shown are indicative and should not be taken to imply perfectly linear relationships. All error bars are 2σ.

in terms of mixing between northern- and southern-sourced waters [*Adkins et al.*, 1998; *Schroder-Ritzrau et al.*, 2003; *Robinson et al.*, 2005; *Thornalley et al.*, 2011b]. In the following discussion, we provide constraints from Nd isotopes on the deglacial mid-depth radiocarbon evolution and assess the extent to which our mixing scenario described for Nd isotopes also applies to the combined Nd isotope and radiocarbon data set.

In Figure 7a, we present a crossplot of ε_{Nd} and $\Delta\Delta^{14}C$ in corals from the New England Seamounts. For comparison to the modern scenario, $\Delta\Delta^{14}C$ in corals is calculated as the offset of the decay-corrected coral $\Delta^{14}C$ from the contemporaneous atmospheric $\Delta^{14}C$ based on IntCal13 [*Reimer et al.*, 2013]. Focusing on the mid-depth (1.7–2.6 km) corals, and considering age groupings, two different trends may be identified (Figure 7b). These corals record similar behavior during the periods 14.9–15.1 ka (red) and 15.7–15.8 ka (blue), and distinct behavior during the period 15.4–15.5 ka (green). In Figure 8, we identify three regions of the crossplot that encapsulate those mid-depth coral data and which also represent the endpoints of those trends. Our first-order observation is that most of those data fall below the modern mixing line between NADW and southern-sourced waters (blue mixing envelope in Figure 8), indicating generally more depleted radiocarbon for a given Nd isotopic composition. Furthermore, those data do not describe either a linear or curved relationship, a result which is inconsistent with simple two-component mixing between northern-sourced and southern-sourced water masses with fixed compositions. In contrast, the shallower corals (1.1–1.4 km) record relatively undepleted radiocarbon compositions, similar to the modern water column at these depths, and their ε_{Nd}-$\Delta\Delta^{14}C$ compositions may be explained by two-component mixing between well-ventilated thermocline waters and northern-sourced waters similar to today (Figure 8). This scenario is consistent with their location close to that hydrographic front in the modern ocean (Figure 2) and our earlier suggestion from Nd isotopes that some thickening of the thermocline may have occurred at times in the past.

For a fuller understanding of the mid-depth variability, we consider below the three regions of the crossplot (Figure 8) in more detail: (i) ε_{Nd} of −11 to −12 and $\Delta\Delta^{14}C$ of −120 to −180; (ii) less radiogenic ε_{Nd} values (−13.5 to −14.5) accompanied by relatively depleted $\Delta\Delta^{14}C$ (−140 to −190); (iii) somewhat less radiogenic ε_{Nd} values (−11.5 to −13) accompanied by highly depleted $\Delta\Delta^{14}C$ (−200 to −240).

5.4.1. Region (i)

Region (i) is closest to the modern mixing envelope (Figure 8) and based on Nd isotopes appears to represent the southern-sourced waters in the North Atlantic Ocean (Figure 6). As described above, the Nd isotopic composition is similar to that recorded at the deep Bermuda Rise [*Roberts et al.*, 2010] but does not represent a pure southern end-member, suggesting significant mixing with Atlantic waters (or non-conservative behavior) has occurred along its northward flow path. These waters are only somewhat more depleted in radiocarbon than in the modern day, consistent with evidence that $\Delta\Delta^{14}C$ of AAIW during the deglacial period was similar to its values in the modern ocean [*de Pol-Holz et al.*, 2010; *Sortor and Lund*, 2011; *Burke and Robinson*, 2012].

5.4.2. Region (ii)

Region (ii) describes waters with an unradiogenic Nd isotopic signature (ε_{Nd} ~ −14) (Figure 8) that is characteristic of northern-sourced waters today, but with a relatively depleted radiocarbon signature, ~170‰ below the atmospheric value. In particular, the Nd isotopes correspond to modern Upper NADW, suggesting that the unradiogenic Nd and depleted radiocarbon may have originated in the Labrador Sea. Another possibility is that open ocean convection in the North Atlantic, which may have been more important during the glacial period [*Boyle and Keigwin*, 1987; *Labeyrie et al.*, 1992], generated a water mass (GNAIW) with an unradiogenic Nd isotope signature that reflected surface water compositions in the subpolar gyre (ε_{Nd} ~ −15) [*Lacan and Jeandel*, 2004a]. If indeed these radiocarbon-depleted waters do have a northern-source, then this result differs from the prediction that depleted radiocarbon would be associated with a southern-source [*Robinson et al.*, 2005]. The alternative explanation is that the northern-sourced water mass end-member had a markedly unradiogenic Nd isotopic composition compared to today, which would require an important role for unradiogenic lithogenic Nd sources located in the Canadian Shield and Baffin Bay [*Jeandel et al.*, 2007]. Both of these options are discussed below.

If the glacial northern-sourced waters remained as well ventilated with respect to radiocarbon as in the modern ocean, we must invoke a change of ~5 ε_{Nd} units in their Nd isotopic composition to approximately −19. A potential source for such an unradiogenic signature is the Labrador Sea (i.e., Baffin Bay) because the surrounding lithology has Nd isotopic compositions of approximately −15 to −30 [*Jeandel et al.*, 2007]. Modern Labrador Sea Water has a Nd isotopic composition of approximately −14.5, so a significant change in continental weathering inputs or boundary exchange would be required to generate such a large shift, which could potentially have been related to deglacial ice sheet variability and retreat and related changes in sediment inputs. Unfortunately, there are no direct constraints on the past composition of Labrador Sea Water on the relevant timescales. Our study also does not provide direct evidence for a change in the Labrador Sea Water end-member because none of our coral data record Nd isotopes that are any less radiogenic than the range of the modern water column (Figure 2). Some evidence for such variability may be found in the early Holocene section of the deep Bermuda Rise Nd isotope record [*Roberts et al.*, 2010], where the most extreme values of −16.5 may have been related to a Labrador Sea signature, although considering the quite different boundary conditions of the deglacial period, this evidence is unlikely to be directly applicable to the question here. Modeling approaches have also addressed the end-member question but have not predicted end-member changes as large as ~5 ε_{Nd} units, even with major variations of the boundary exchange or riverine sources [*Rempfer et al.*, 2012]. Nevertheless, since observational data cannot rule out large end-member changes in Labrador Sea Water, we suggest that constraining past changes in this end-member will be an important target for future studies.

If instead the Nd isotopic composition of the northern-sourced waters remained constant, or did not change markedly from today, we must invoke a change in their radiocarbon composition towards more depleted values. For a northern-sourced water mass to have a radiocarbon-depleted signature requires that it formed under somewhat different conditions than NADW today. Possible explanations for radiocarbon depletion could include (a) formation under sea ice which hinders exchange with the atmosphere; (b) formation from upwelled subsurface waters supplying depleted radiocarbon; (c) a longer residence time of deep waters in an upstream basin before export into the Atlantic basin; or (d) a slower transport time within the Atlantic basin

itself. We exclude a long residence time of deep waters in an upstream basin because the Labrador Sea is not a silled basin, while such an explanation would also not apply to a scenario with open ocean convection. A slow transport time in the Atlantic Ocean also seems unlikely because of the proximity of the New England Seamounts to the inferred source locations to the north, the steep Nd isotope gradients between the mid-depth and deep oceans, which in combination with multiple and rapid changes may imply strong lateral advection (Figure 6), and the evidence from $^{231}Pa/^{230}Th$ for ongoing Atlantic overturning at mid-depths during the deglaciation [*Gherardi et al.*, 2009].

In contrast, a source effect (due to sea ice expansion or upwelled subsurface waters) appears most feasible in light of evidence for old radiocarbon in the deglacial North Atlantic surface ocean [*Waelbroeck et al.*, 2001; *Peck et al.*, 2006; *Thornalley et al.*, 2011a; *Stern and Lisiecki*, 2013]. For example, surface reservoir ages as large as ~1–2 kyr (compared to ~400 years in the modern day) have been reconstructed for late Heinrich Stadial 1 in the open North Atlantic north of 40°N [*Waelbroeck et al.*, 2001; *Thornalley et al.*, 2011a]. While a recent assessment suggests that reservoir ages of ~1.0–1.3 kyr during Heinrich Stadial 1 declined after 16 ka to ~500–700 years [*Stern and Lisiecki*, 2013], these ages are still significantly older than in the modern day. Regardless of the mechanism(s) behind the radiocarbon depletion, our combined Nd isotope and radiocarbon data are consistent with a possible North Atlantic source of depleted radiocarbon during the deglaciation.

5.4.3. Region (iii): The 15.4 ka Event

Region (iii) only applies to the transient ε_{Nd}-$\Delta\Delta^{14}C$ evolution at ~15.4 ka and differs from the prior discussion in requiring an even more radiocarbon-depleted signature to accompany a somewhat unradiogenic ε_{Nd} signature (Figure 8). Therefore, we suggest that different water mass sources (or source signatures) were present during this event than at other times during Heinrich Stadial 1. A very rapid change in ventilation was inferred for the ~15.4 ka event from coral transect data [*Adkins et al.*, 1998], which rules out that the depleted radiocarbon signatures could be due simply to ageing with reduced Atlantic transport producing a stagnant mid-depth water mass [*Adkins et al.*, 1998; *Robinson et al.*, 2005]. In those previous studies, a switch in water mass sourcing and/or mixing was proposed to explain the changes, with depleted radiocarbon linked to incursion of a southern-sourced water mass [*Adkins et al.*, 1998; *Robinson et al.*, 2005]. However, we now show that the radiocarbon changes were not accompanied by large changes in Nd isotopes (e.g., transect JFA24.8; Figures 5b and 7b). That transect is important because it rules out a simple switch from northern- to southern-sourced waters as the mechanism behind radiocarbon depletion during the 15.4 ka event. Instead, the data may be explained by the presence of three or more water masses in the Atlantic Ocean at that time (Figure 8). Below we describe three possible scenarios for the radiocarbon depletion during the ~15.4 ka event.

The first possibility is that the radiocarbon-depleted signature at ~15.4 ka has a northern origin. Although the ε_{Nd} values of −11.5 to −12.8 are too radiogenic to represent modern-like Upper NADW (Figure 2), they could indicate mixing towards a water mass comparable to modern-day Middle NADW, originating from the Greenland-Iceland-Norwegian Seas with only minimal entrainment of the unradiogenic Labrador Sea Water. Such an aged radiocarbon signature could have been generated in the Greenland-Iceland-Norwegian Seas, where there is evidence for highly variable surface reservoir ages during the late glacial and deglacial periods, at times in excess of 2 kyr [*Voelker et al.*, 1998]. In particular, surface reservoir ages of at least 1.2 kyr are reported from the Norwegian Sea at 15 ka during late Heinrich Stadial 1 [*Bjorck et al.*, 2003], indicating reduced atmosphere-ocean exchange at this time. Deep storage and decay of radiocarbon could also have occurred in that silled basin before the water overflowed to become incorporated into the mid-depth Atlantic basin. Intermediate water formation in the Norwegian Sea was highly variable towards the end of the last glacial period, with millennial and centennial changes in ventilation [*Rorvik et al.*, 2013], indicating also the potential for changes over short timescales as required by the deep-sea coral data. Deep water formation by brine rejection has also been invoked to explain anomalously light oxygen and carbon isotopes in the Norwegian Seas during Heinrich Stadial 1 [*Dokken and Jansen*, 1999] and such a water mass may have been exported into the intermediate to mid-depth North Atlantic [*Meland et al.*, 2008; *Waelbroeck et al.*, 2011], providing a radiocarbon-depleted source to both the northeast Atlantic [*Thornalley et al.*, 2011b] and the New England Seamounts.

A second possibility for the radiocarbon changes during the ~15.4 ka event involves a change in the radiocarbon content of the southern-sourced waters at the New England Seamounts (Figure 8). Since AAIW had a largely unchanging $\Delta\Delta^{14}C$ during the deglacial period that was similar to its values in the modern

ocean [*de Pol-Holz et al.*, 2010; *Sortor and Lund*, 2011; *Burke and Robinson*, 2012], we suggest that a southern source of highly depleted radiocarbon at the New England Seamounts could only have originated in the deeper southern-sourced waters (i.e., AABW). One intriguing possibility here is that the better ventilated AAIW represented the southern end-member in region (i) and that region (iii) records a switch to a poorly ventilated glacial AABW source [*Skinner et al.*, 2010; *Burke and Robinson*, 2012] during the ~15.4 ka event (Figure 8). At present, we do not attempt to distinguish between these two different hypotheses for changing sources (i.e., Greenland-Iceland-Norwegian Sea versus an AAIW/AABW switch) and we suggest that comparable data from more locations within the Atlantic Ocean may be required to test them.

Finally, we suggest a third possibility, that the 15.4 ka corals are sampling a different part of the mixing diagram for ε_{Nd} and $\Delta^{14}C$. Region (iii) in Figure 8 could be the result of mixing between northern and southern end-members, similar to region (i), but at a slower circulation rate, thereby allowing $\Delta^{14}C$ to deviate more strongly from conservative mixing. This slower circulation could have been strongly depth-dependent in the deglacial Atlantic water column, and indeed, we might require this since we have already provided evidence for highly dynamic circulation changes at the mid-depths sampled by the corals. It is possible, therefore, that the ~15.4 ka event differs from the other two large Nd isotope excursions by being a vertical movement of water mass fronts, rather than a horizontal movement due to competition between northern and southern water masses at intermediate depths. Such slow circulation at depth, accompanied by radiocarbon decay, and followed by upward mixing towards shallower depths in the latter part of Heinrich Stadial 1 is rather similar to the recent hypothesis of *Meckler et al.* [2013]. However, we emphasize again that distinguishing between the various scenarios presented here will require a more complete spatial-temporal data set for the deglacial Atlantic.

The preceding discussion highlights both the value and complexity of combining multiple tracers, in this case Nd isotopes and radiocarbon, to better resolve changes in water mass mixing and/or source properties. That aim is complicated by the potential for changes in either or both of the Nd isotope and radiocarbon compositions of the end-members through time. The question of Nd isotope end-members has been discussed above, while it will probably also be challenging to determine the evolution of surface reservoir ages in these regions at a sufficiently high resolution to characterize end-member radiocarbon compositions on millennial timescales. Deep-sea corals from intermediate depths near these water mass source regions may provide improved constraints in the future [e.g., *Lopez Correa et al.*, 2012].

5.5. Ocean Circulation Link to Deglacial Climate Variability

Previous studies have linked North Atlantic warming at the transition into the Bolling-Allerod with changes in the AMOC [*Clark et al.*, 2002], which has been supported by proxies based on both overturning strength [*McManus et al.*, 2004] and water mass mixing [*Roberts et al.*, 2010]. Those studies were based on the deep ocean (~4.5 km) where, in contrast to our study, rapid changes within Heinrich Stadial 1 were not observed. Therefore, while ocean circulation changes affecting the full depth of the Atlantic Ocean may have been related to the warming during the Bolling-Allerod and were perhaps influential in the glacial-interglacial transition, we have provided evidence that the mid-depth circulation changed first during the preceding millennium. Both Nd isotopes and radiocarbon record a very dynamic behavior of the mid-depth ocean during that period before the onset of Bolling-Allerod warming, suggesting that this part of the ocean system may have played an important role in early deglacial climate evolution. Our mid-depth corals from the New England Seamounts may have been sensitively located to record that behavior, rather than recording wholesale changes in the configuration of the overturning circulation.

Additional evidence on the mid-depth North Atlantic hydrography during Heinrich Stadial 1 has recently emerged from clumped isotope measurements on corals from the New England Seamounts [*Thiagarajan et al.*, 2014]. That study demonstrated a mid-depth warming of 3–4°C at ~15.5 ka, producing a water column prone to instabilities and potentially preconditioning the deep ocean for the subsequent Bolling-Allerod circulation switch. Therefore, the radiocarbon depletion of the ~15.4 ka event described above was associated with warm waters, which were postulated to have come from the south. We see a shift towards more radiogenic Nd isotopes from ~15.8 ka to ~15.5 ka, also preceding that radiocarbon depletion, which may support such a southern source for that water. However, as described above, it is not possible to rule out other potential sources (such as a Greenland-Iceland-Norwegian Seas source) for the ~15.4 ka event from Nd isotope evidence alone, and we also cannot rule out that a complex mixture of sources may have been involved.

At this point we have more Nd isotope than clumped isotope data from the New England Seamounts corals, so while there is agreement between the two tracers at ~15.5 ka, there is not yet enough clumped isotope data to compare with the other two rapid events seen in Figure 5b. The other important conclusion of *Thiagarajan et al.* [2014] was that the water column structure was fundamentally different between Heinrich Stadial 1 and the Younger Dryas, reflecting a reorganization at the Bolling-Allerod. That suggestion is supported by the Nd isotope data presented here (Figure 6), although more Nd isotope data from the Younger Dryas would be helpful in this regard.

The Greenland ice core records also show some variability during late Heinrich Stadial 1 (Figure 3), but a detailed comparison to the coral records is not possible, as much due to the uncertainties in ice core chronologies and centennial-scale differences between ice core records [*Svensson et al.*, 2006] as due to the uncertainties in the uranium-series coral ages. At this stage, we can therefore only speculate that the transient ocean circulation events identified at the New England Seamounts may have been linked to basin-wide changes in AMOC and corresponding short-lived warming events in Greenland. Rapid changes have been widely observed in the North Atlantic Ocean during this period, including sea ice fluctuations in the far North Atlantic [*de Vernal et al.*, 2001] and sea surface temperature and salinity variability in the subtropics that was interpreted in terms of an early resumption of shallower overturning preceding the deeper overturning at the Bolling-Allerod [*Carlson et al.*, 2008]. Evidence from carbon isotopes and Nd isotopes in the deep South Atlantic has also been used to argue for a "false start" of NADW production preceding the Bolling-Allerod warming [*Charles and Fairbanks*, 1992; *Piotrowski et al.*, 2004]. Our study provides further evidence in support of those previous suggestions that this was a period of dynamic ocean-climate interaction. At present, we are not able to address whether the Nd isotope variability observed at the New England Seamounts during Heinrich Stadial 1 was restricted to the early deglacial period, and perhaps significant for the deglaciation itself, or whether such variability also characterized previous Heinrich events during the glacial period. Resolving this question would require an extensive and well-dated dataset from marine isotope stage 3.

We finally consider the possible significance of these circulation changes for the carbon cycle evolution during the deglaciation. Glacial carbon storage in the deep oceans and deglacial carbon release is most commonly linked to changes in the Southern Ocean [*Sigman et al.*, 2010; *Skinner et al.*, 2010; *Burke and Robinson*, 2012], and our data from the ~15.4 ka event are not inconsistent with a southern-source of depleted radiocarbon. However, we have also shown that there were times (~15.0 ka and ~15.8 ka) when northern-sourced Nd isotope signatures may have been associated with depleted radiocarbon in the Atlantic, and in addition, our data suggest that a dynamic mid-depth AMOC continued at least transiently during the latter part of Heinrich Stadial 1. Together, this evidence raises the possibility that ventilation of the mid-depth oceans from a northern-source contributed to the increasing atmospheric CO_2 and decreasing $\Delta^{14}C_{atm}$ during the deglacial period [*Broecker and Barker*, 2007], with CO_2 being released to the atmosphere when this water was exported and upwelled in the Southern Ocean.

6. Conclusions

We have used combined radiocarbon and Nd isotopes from deep-sea corals to reconstruct variability in the intermediate to mid-depth North Atlantic water column across the last deglaciation. In particular, the high temporal resolution during the latter half of Heinrich Stadial 1 has provided evidence for a highly dynamic behavior at this time. Rapid fluctuations of water mass sourcing and radiocarbon affected the mid-depth water column (1.7–2.5 km) before the onset of the Bolling-Allerod warming, at a time with minimal changes in the deep North Atlantic. This evidence is inconsistent with a complete shutdown of the AMOC throughout Heinrich Stadial 1 and, whereas AMOC changes affecting the whole water column were probably important for North Atlantic climate variability during the Bolling-Allerod warming, changes in the AMOC at intermediate depths may have been important during earlier stages of the deglaciation.

In detail, our new data reveal that mixing relationships during the deglaciation were complex and a two-component mixing model, between well-ventilated northern-sourced and radiocarbon-depleted southern-sourced water masses similar to today, cannot explain all our data. For example, at ~15.8 ka and ~15.0 ka, ε_{Nd} values ≤ -14 suggest contributions from Labrador Sea Water and/or open ocean convection south of Greenland, and were associated with a radiocarbon reservoir age of up to 1 kyr. Unless there were significant

changes in the Nd isotopic composition of the northern end-member, these data imply that the northern-sourced waters had relatively depleted radiocarbon at this time. In addition, rapid shifts towards the most depleted radiocarbon are observed during the ~15.4 ka event but are only associated with small changes in Nd isotopes towards $\varepsilon_{Nd} \sim -12$. A number of explanations are possible for this event, including (a) deep water sourced in the Greenland-Iceland-Norwegian Seas, possibly by brine rejection; (b) a switch to mixing with a more radiocarbon-depleted southern-sourced deep water mass at this time; or (c) a vertical frontal movement leading to the temporary influence of a slow deep circulation regime. However, neodymium isotopes alone are unable to further resolve the origin of that depleted radiocarbon signature.

Although we have focused on the possibility of different radiocarbon signatures for northern-sourced waters during the deglacial period, our study has also reopened the question of variability of the northern end-member in Nd isotopes. If the Nd isotope variability we observe on short timescales is the result of significant water mass changes at these depths, then we are limited in our ability to assess the Nd isotopic composition of the northern-sourced end-member from records in this region. Alternatively, the observed Nd isotopic variability could reflect, at least in part, variations in that end-member. In either case, the idea of a constant NADW end-member [cf. *van de Flierdt et al.*, 2006; *Foster et al.*, 2007] may need to be revised, in particular when short timescales are considered. This question remains an important area for future research.

More generally, our study has highlighted the unique value of deep-sea corals as a paleoceanographic archive in a number of ways: (i) they provide absolute and relatively precise uranium-series ages with potential for high-resolution studies; (ii) they are a suitable archive for combined Nd isotope and radiocarbon reconstructions to be made on the same carbonate phase; and (iii) they grow in locations such as the intermediate to mid-depth oceans where sediment cores are not always available and where there appears to have been rapid oceanographic variability. We therefore envisage great potential in future studies of radiogenic isotope tracers in deep-sea corals.

Acknowledgments

Data to support this article are provided in Table 1 and Table S1 in the supporting information. This study was supported by Natural Environment Research Council grant NE/F016751/1, Marie Curie International Reintegration grant IRG 230828, and Leverhulme Trust grant RPG-398 to TvdF, as well as a Phillip Leverhulme Prize, Marie Curie International Reintegration Grant, and European Research Council grant to L.F.R. We are grateful for thoughtful reviews from Marcus Gutjahr and an anonymous reviewer and the editorial handling by Heiko Pälike.

References

Adkins, J. F., and E. A. Boyle (1999), Age screening of deep-sea corals and the record of deep north Atlantic circulation change at 15.4 ka, in *Reconstructing Ocean History: A Window Into the Future*, edited by F. Abrantes and A. C. Mix, pp. 103–120, Kluwer Academic/Plenum Publ., New York.

Adkins, J. F., H. Cheng, E. A. Boyle, E. R. M. Druffel, and R. L. Edwards (1998), Deep-sea coral evidence for rapid change in ventilation of the deep North Atlantic 15,400 years ago, *Science*, *280*(5364), 725–728.

Adkins, J. F., G. M. Henderson, S. L. Wang, S. O'Shea, and F. Mokadem (2004), Growth rates of the deep-sea scleractinia *Desmophyllum cristagalli* and *Enallopsammia rostrata*, *Earth Planet. Sci. Lett.*, *227*(3–4), 481–490.

Arsouze, T., J. C. Dutay, F. Lacan, and C. Jeandel (2009), Reconstructing the Nd oceanic cycle using a coupled dynamical-biogeochemical model, *Biogeosciences*, *6*(12), 2829–2846.

Barker, S., G. Knorr, M. J. Vautravers, P. Diz, and L. C. Skinner (2010), Extreme deepening of the Atlantic overturning circulation during deglaciation, *Nat. Geosci.*, *3*(8), 567–571.

Bjorck, S., N. Koc, and G. Skog (2003), Consistently large marine reservoir ages in the Norwegian Sea during the Last Deglaciation, *Quat. Sci. Rev.*, *22*(5–7), 429–435.

Boyle, E. A., and L. Keigwin (1987), North Atlantic thermohaline circulation during the past 20,000 years linked to high-latitude surface temperature, *Nature*, *330*(6143), 35–40.

Broecker, W., and S. Barker (2007), A 190 permil drop in atmosphere's $\Delta^{14}C$ during the "Mystery Interval" (17.5 to 14.5 kyr), *Earth Planet. Sci. Lett.*, *256*(1–2), 90–99.

Broecker, W. S., and G. H. Denton (1989), The role of ocean-atmosphere reorganizations in glacial cycles, *Geochim. Cosmochim. Acta*, *53*(10), 2465–2501.

Broecker, W. S., G. H. Denton, R. L. Edwards, H. Cheng, R. B. Alley, and A. E. Putnam (2010), Putting the Younger Dryas cold event into context, *Quat. Sci. Rev.*, *29*(9–10), 1078–1081.

Burke, A., and L. F. Robinson (2012), The Southern Ocean's role in carbon exchange during the last deglaciation, *Science*, *335*(6068), 557–561.

Burke, A., O. Marchal, L. I. Bradtmiller, J. F. McManus, and R. Francois (2011), Application of an inverse method to interpret $^{231}Pa/^{230}Th$ observations from marine sediments, *Paleoceanography*, *26*, PA1212, doi:10.1029/2010PA002022.

Came, R. E., D. W. Oppo, W. B. Curry, and J. Lynch-Stieglitz (2008), Deglacial variability in the surface return flow of the Atlantic meridional overturning circulation, *Paleoceanography*, *23*, PA1217, doi:10.1029/2007PA001450.

Carlson, A. E., D. W. Oppo, R. E. Came, A. N. LeGrande, L. D. Keigwin, and W. B. Curry (2008), Subtropical Atlantic salinity variability and Atlantic meridional circulation during the last deglaciation, *Geology*, *36*(12), 991–994.

Charles, C. D., and R. G. Fairbanks (1992), Evidence from Southern Ocean sediments for the effect of North Atlantic deep-water flux on climate, *Nature*, *355*(6359), 416–419.

Chase, Z., R. F. Anderson, M. Q. Fleisher, and P. W. Kubik (2002), The influence of particle composition and particle flux on scavenging of Th, Pa and Be in the ocean, *Earth Planet. Sci. Lett.*, *204*(1–2), 215–229.

Cheng, H., J. Adkins, R. L. Edwards, and E. A. Boyle (2000), U-Th dating of deep-sea corals, *Geochim. Cosmochim. Acta*, *64*(14), 2401–2416.

Clark, P. U., N. G. Pisias, T. F. Stocker, and A. J. Weaver (2002), The role of the thermohaline circulation in abrupt climate change, *Nature*, *415*(6874), 863–869.

Clark, P. U., et al. (2012), Global climate evolution during the last deglaciation, *Proc. Natl. Acad. Sci. U.S.A.*, *109*(19), E1134–E1142.

Colin, C., N. Frank, K. Copard, and E. Douville (2010), Neodymium isotopic composition of deep-sea corals from the NE Atlantic: Implications for past hydrological changes during the Holocene, *Quat. Sci. Rev.*, *29*(19–20), 2509–2517.

Copard, K., C. Colin, E. Douville, A. Freiwald, G. Gudmundsson, B. De Mol, and N. Frank (2010), Nd isotopes in deep-sea corals in the North-eastern Atlantic, *Quat. Sci. Rev.*, *29*(19–20), 2499–2508.

Crocket, K. C., M. Lambelet, T. van de Flierdt, M. Rehkamper, and L. F. Robinson (2014), Measurement of fossil deep-sea coral Nd isotopic compositions and concentrations by TIMS as NdO^+, with evaluation of cleaning protocols, *Chem. Geol.*, *374–375*, 128–140.

Curry, W. B., and D. W. Oppo (2005), Glacial water mass geometry and the distribution of $\delta^{13}C$ of ΣCO_2 in the western Atlantic Ocean, *Paleoceanography*, *20*, PA1017, doi:10.1029/2004PA001021.

Dansgaard, W., et al. (1993), Evidence for general instability of past climate from a 250-kyr ice-core record, *Nature*, *364*(6434), 218–220.

de Pol-Holz, R., L. Keigwin, J. Southon, D. Hebbeln, and M. Mohtadi (2010), No signature of abyssal carbon in intermediate waters off Chile during deglaciation, *Nat. Geosci.*, *3*(3), 192–195.

de Vernal, A., et al. (2001), Dinoflagellate cyst assemblages as tracers of sea-surface conditions in the northern North Atlantic, Arctic and sub-Arctic seas: The new "n = 677" data base and its application for quantitative palaeoceanographic reconstruction, *J. Quat. Sci.*, *16*(7), 681–698.

Dokken, T. M., and E. Jansen (1999), Rapid changes in the mechanism of ocean convection during the last glacial period, *Nature*, *401*(6752), 458–461.

Elmore, A. C., A. M. Piotrowski, J. D. Wright, and A. E. Scrivner (2011), Testing the extraction of past seawater Nd isotopic composition from North Atlantic deep sea sediments and foraminifera, *Geochem. Geophys. Geosyst.*, *12*, Q09008, doi:10.1029/2011GC003741.

Eltgroth, S. F., J. F. Adkins, L. F. Robinson, J. Southon, and M. Kashgarian (2006), A deep-sea coral record of North Atlantic radiocarbon through the Younger Dryas: Evidence for intermediate water/deepwater reorganization, *Paleoceanography*, *21*, PA4207, doi:10.1029/2005PA001192.

Foster, G. L., D. Vance, and J. Prytulak (2007), No change in the neodymium isotope composition of deep water exported from the North Atlantic on glacial-interglacial time scales, *Geology*, *35*(1), 37–40.

Frank, M. (2002), Radiogenic isotopes: Tracers of past ocean circulation and erosional input, *Rev. Geophys.*, *40*(1), 1001, doi:10.1029/2000RG000094.

Gherardi, J. M., L. Labeyrie, S. Nave, R. Francois, J. F. McManus, and E. Cortijo (2009), Glacial-interglacial circulation changes inferred from $^{231}Pa/^{230}Th$ sedimentary record in the North Atlantic region, *Paleoceanography*, *24*, PA2204, doi:10.1029/2008PA001696.

Goldstein, S. L., and S. R. Hemming (2003), Long-lived isotopic tracers in oceanography, paleoceanography and ice sheet dynamics, in *The Oceans and Marine Geochemistry*, edited by H. Elderfield, pp. 453–489, Elsevier-Pergamon, Oxford, U. K.

Grootes, P. M., M. Stuiver, J. W. C. White, S. Johnsen, and J. Jouzel (1993), Comparison of oxygen isotope records from the GISP2 and GRIP Greenland ice cores, *Nature*, *366*(6455), 552–554.

Gutjahr, M., and J. Lippold (2011), Early arrival of Southern-source Water in the deep North Atlantic prior to Heinrich event 2, *Paleoceanography*, *26*, PA2101, doi:10.1029/2011PA002114.

Gutjahr, M., M. Frank, C. H. Stirling, L. D. Keigwin, and A. N. Halliday (2008), Tracing the Nd isotope evolution of North Atlantic deep and intermediate waters in the Western North Atlantic since the Last Glacial Maximum from Blake Ridge sediments, *Earth Planet. Sci. Lett.*, *266*(1–2), 61–77.

Hain, M. P., D. M. Sigman, and G. H. Haug (2014), Distinct roles of the Southern Ocean and North Atlantic in the deglacial atmospheric radiocarbon decline, *Earth Planet. Sci. Lett.*, *394*, 198–208.

Hayes, C. T., R. F. Anderson, M. Q. Fleisher, K. F. Huang, L. F. Robinson, Y. Lu, H. Cheng, R. L. Edwards, and S. B. Moranh (2014), ^{230}Th and ^{231}Pa on GEOTRACES GA03, the U.S. GEOTRACES North Atlantic transect, and implications for modern and paleoceanographic chemical fluxes, *Deep Sea Res. Part II Topic. Stud. Oceanogr.*, doi:10.1016/j.dsr1012.2014.1007.1007.

Hemming, S. R. (2004), Heinrich events: Massive late pleistocene detritus layers of the North Atlantic and their global climate imprint, *Rev. Geophys.*, *42*, RG1005, doi:10.1029/2003RG000128.

Hendry, K. R., L. F. Robinson, J. F. McManus, and J. D. Hays (2014), Silicon isotopes indicate enhanced carbon export efficiency in the North Atlantic during deglaciation, *Nat. Commun.*, *5*(3107), doi:10.1038/ncomms4107.

Huang, K. F., D. W. Oppo, and W. B. Curry (2014), Decreased influence of Antarctic intermediate water in the tropical Atlantic during North Atlantic cold events, *Earth Planet. Sci. Lett.*, *389*, 200–208.

Imbrie, J., et al. (1992), On the structure and origin of major glaciation cycles 1. Linear responses to Milankovitch forcing, *Paleoceanography*, *7*(6), 701–738, doi:10.1029/92PA02253.

Jacobsen, S. B., and G. J. Wasserburg (1980), Sm-Nd isotopic composition of chondrites, *Earth Planet. Sci. Lett.*, *50*(1), 139–155.

Jeandel, C. (1993), Concentration and isotopic composition of Nd in the South Atlantic Ocean, *Earth Planet. Sci. Lett.*, *117*(3–4), 581–591.

Jeandel, C., T. Arsouze, F. Lacan, P. Techine, and J. C. Dutay (2007), Isotopic Nd compositions and concentrations of the lithogenic inputs into the ocean: A compilation, with an emphasis on the margins, *Chem. Geol.*, *239*(1–2), 156–164.

Johnsen, S. J., H. B. Clausen, W. Dansgaard, K. Fuhrer, N. Gundestrup, C. U. Hammer, P. Iversen, J. Jouzel, B. Stauffer, and J. P. Steffensen (1992), Irregular glacial interstadials recorded in a new Greenland ice core, *Nature*, *359*(6393), 311–313.

Kraft, S., M. Frank, E. C. Hathorne, and S. Weldeab (2013), Assessment of seawater Nd isotope signatures extracted from foraminiferal shells and authigenic phases of Gulf of Guinea sediments, *Geochim. Cosmochim. Acta*, *121*, 414–435.

Labeyrie, L. D., J. C. Duplessy, J. Duprat, A. Juilletleclerc, J. Moyes, E. Michel, N. Kallel, and N. J. Shackleton (1992), Changes in the vertical structure of the North Atlantic Ocean between glacial and modern times, *Quat. Sci. Rev.*, *11*(4), 401–413.

Lacan, F., and C. Jeandel (2004a), Subpolar Mode Water formation traced by neodymium isotopic composition, *Geophys. Res. Lett.*, *31*, L14306, doi:10.1029/2004GL019747.

Lacan, F., and C. Jeandel (2004b), Neodymium isotopic composition and rare earth element concentrations in the deep and intermediate Nordic Seas: Constraints on the Iceland Scotland Overflow Water signature, *Geochem. Geophys. Geosyst.*, *5*, Q11006, doi:10.1029/2004GC000742.

Lacan, F., and C. Jeandel (2005a), Neodymium isotopes as a new tool for quantifying exchange fluxes at the continent-ocean interface, *Earth Planet. Sci. Lett.*, *232*(3–4), 245–257.

Lacan, F., and C. Jeandel (2005b), Acquisition of the neodymium isotopic composition of the North Atlantic Deep Water, *Geochem. Geophys. Geosyst.*, *6*, doi:10.1029/2005GC000956.

Lambelet, M., T. van de Flierdt, K. Crocket, M. Rehkamper, and H. de Baar (2014), The neodymium isotopic composition of North Atlantic Deep Water revisited, *Ocean Sciences Conference, Abstract ID 16362*, February 2014.

Lopez Correa, M., P. Montagna, N. Joseph, A. Ruggeberg, J. Fietzke, S. Flogel, B. Dorschel, S. L. Goldstein, A. Wheeler, and A. Freiwald (2012), Preboreal onset of cold-water coral growth beyond the Arctic Circle revealed by coupled radiocarbon and U-series dating and neodymium isotopes, *Quat. Sci. Rev.*, *34*, 24–43.

Lynch-Stieglitz, J., et al. (2007), Atlantic meridional overturning circulation during the Last Glacial Maximum, *Science*, *316*(5821), 66–69.

Marchitto, T. M., and W. S. Broecker (2006), Deep water mass geometry in the glacial Atlantic Ocean: A review of constraints from the paleonutrient proxy Cd/Ca, *Geochem. Geophys. Geosyst.*, *7*, Q12003, doi:10.1029/2006GC001323.

McManus, J. F., R. Francois, J. M. Gherardi, L. D. Keigwin, and S. Brown-Leger (2004), Collapse and rapid resumption of Atlantic meridional circulation linked to deglacial climate changes, *Nature*, *428*(6985), 834–837.
Meckler, A. N., D. M. Sigman, K. A. Gibson, R. Francois, A. Martinez-Garcia, S. L. Jaccard, U. Rohl, L. C. Peterson, R. Tiedemann, and G. H. Haug (2013), Deglacial pulses of deep-ocean silicate into the subtropical North Atlantic Ocean, *Nature*, *495*(7442), 495–498.
Meland, M. Y., T. M. Dokken, E. Jansen, and K. Hevroy (2008), Water mass properties and exchange between the Nordic seas and the northern North Atlantic during the period 23–6 ka: Benthic oxygen isotopic evidence, *Paleoceanography*, *23*, PA1210, doi:10.1029/2007PA001416.
Pahnke, K., S. L. Goldstein, and S. R. Hemming (2008), Abrupt changes in Antarctic Intermediate Water circulation over the past 25,000 years, *Nat. Geosci.*, *1*(12), 870–874.
Peck, V. L., I. R. Hall, R. Zahn, H. Elderfield, F. Grousset, S. R. Hemming, and J. D. Scourse (2006), High resolution evidence for linkages between NW European ice sheet instability and Atlantic Meridional Overturning Circulation, *Earth Planet. Sci. Lett.*, *243*(3–4), 476–488.
Piepgras, D. J., and G. J. Wasserburg (1987), Rare earth element transport in the western North Atlantic inferred from Nd isotopic observations, *Geochim. Cosmochim. Acta*, *51*(5), 1257–1271.
Piotrowski, A. M., S. L. Goldstein, S. R. Hemming, and R. G. Fairbanks (2004), Intensification and variability of ocean thermohaline circulation through the last deglaciation, *Earth Planet. Sci. Lett.*, *225*(1–2), 205–220.
Piotrowski, A. M., A. Galy, J. A. L. Nicholl, N. Roberts, D. J. Wilson, J. A. Clegg, and J. Yu (2012), Reconstructing deglacial North and South Atlantic deep water sourcing using foraminiferal Nd isotopes, *Earth Planet. Sci. Lett.*, *357*, 289–297.
Reimer, P. J., et al. (2013), IntCal13 and Marine13 radiocarbon age calibration curves 0–50,000 years cal BP, *Radiocarbon*, *55*(4), 1869–1887.
Rempfer, J., T. F. Stocker, F. Joos, J. C. Dutay, and M. Siddall (2011), Modelling Nd-isotopes with a coarse resolution ocean circulation model: Sensitivities to model parameters and source/sink distributions, *Geochim. Cosmochim. Acta*, *75*(20), 5927–5950.
Rempfer, J., T. F. Stocker, F. Joos, and J. C. Dutay (2012), Sensitivity of Nd isotopic composition in seawater to changes in Nd sources and paleoceanographic implications, *J. Geophys. Res.*, *117*, C12010, doi:10.1029/2012JC008161.
Rickaby, R. E. M., and H. Elderfield (2005), Evidence from the high-latitude North Atlantic for variations in Antarctic Intermediate water flow during the last deglaciation, *Geochem. Geophys. Geosyst.*, *6*, Q05001, doi:10.1029/2004GC000858.
Roberts, N. L., A. M. Piotrowski, J. F. McManus, and L. D. Keigwin (2010), Synchronous deglacial overturning and water mass source changes, *Science*, *327*(5961), 75–78.
Robinson, L. F., and T. van de Flierdt (2009), Southern Ocean evidence for reduced export of North Atlantic Deep Water during Heinrich event 1, *Geology*, *37*(3), 195–198.
Robinson, L. F., J. F. Adkins, L. D. Keigwin, J. Southon, D. P. Fernandez, S. L. Wang, and D. S. Scheirer (2005), Radiocarbon variability in the western North Atlantic during the last deglaciation, *Science*, *310*(5753), 1469–1473.
Robinson, L. F., J. F. Adkins, D. S. Scheirer, D. P. Fernandez, A. Gagnon, and R. G. Waller (2007), Deep-sea scleractinian coral age and depth distributions in the northwest Atlantic for the last 225,000 years, *Bull. Mar. Sci.*, *81*(3), 371–391.
Robinson, L. F., J. F. Adkins, N. Frank, A. C. Gagnon, N. G. Prouty, E. B. Roark, and T. van de Flierdt (2014), The geochemistry of deep-sea coral skeletons: A review of vital effects and applications for palaeoceanography, *Deep Sea Res. Part II Topic. Stud. Oceanogr.*, *99*, 184–198.
Rorvik, K. L., T. L. Rasmussen, M. Hald, and K. Husum (2013), Intermediate water ventilation in the Nordic seas during MIS 2, *Geophys. Res. Lett.*, *40*, 1805–1810, doi:10.1002/grl.50325.
Rutberg, R. L., S. R. Hemming, and S. L. Goldstein (2000), Reduced North Atlantic Deep Water flux to the glacial Southern Ocean inferred from neodymium isotope ratios, *Nature*, *405*(6789), 935–938.
Sarnthein, M., and R. Tiedemann (1990), Younger Dryas-style cooling events at glacial terminations I-VI at ODP Site 658: Associated benthic $\delta^{13}C$ anomalies constrain meltwater hypothesis, *Paleoceanography*, *5*(6), 1041–1055, doi:10.1029/PA005i006p01041.
Schmitz, W. J., Jr. (1996), *On the World Ccean Circulation: Volume I: Some Global Features/North Atlantic Circulation*, Woods Hole Oceanographic Institute, Woods Hole, Mass.
Schroder-Ritzrau, A., A. Mangini, and M. Lomitschka (2003), Deep-sea corals evidence periodic reduced ventilation in the North Atlantic during the LGM/Holocene transition, *Earth Planet. Sci. Lett.*, *216*(3), 399–410.
Severinghaus, J. P., and E. J. Brook (1999), Abrupt climate change at the end of the last glacial period inferred from trapped air in polar ice, *Science*, *286*(5441), 930–934.
Siddall, M., S. Khatiwala, T. van de Flierdt, K. Jones, S. L. Goldstein, S. Hemming, and R. F. Anderson (2008), Towards explaining the Nd paradox using reversible scavenging in an ocean general circulation model, *Earth Planet. Sci. Lett.*, *274*(3–4), 448–461.
Sigman, D. M., M. P. Hain, and G. H. Haug (2010), The polar ocean and glacial cycles in atmospheric CO_2 concentration, *Nature*, *466*(7302), 47–55.
Skinner, L. C., and N. J. Shackleton (2004), Rapid transient changes in northeast Atlantic deep water ventilation age across Termination I, *Paleoceanography*, *19*, PA2005, doi:10.1029/2003PA000983.
Skinner, L. C., N. J. Shackleton, and H. Elderfield (2003), Millennial-scale variability of deep-water temperature and $\delta^{18}O_{dw}$ indicating deep-water source variations in the Northeast Atlantic, 0-34 cal. ka BP, *Geochem. Geophys. Geosyst.*, *4*(12), 1098, doi:10.1029/2003GC000585.
Skinner, L. C., S. Fallon, C. Waelbroeck, E. Michel, and S. Barker (2010), Ventilation of the deep Southern Ocean and deglacial CO_2 rise, *Science*, *328*(5982), 1147–1151.
Sortor, R. N., and D. C. Lund (2011), No evidence for a deglacial intermediate water $\Delta^{14}C$ anomaly in the SW Atlantic, *Earth Planet. Sci. Lett.*, *310*(1–2), 65–72.
Stern, J. V., and L. E. Lisiecki (2013), North Atlantic circulation and reservoir age changes over the past 41,000years, *Geophys. Res. Lett.*, *40*, 3693–3697, doi:10.1002/grl.50679.
Stichel, T., M. Frank, J. Rickli, and B. A. Haley (2012), The hafnium and neodymium isotope composition of seawater in the Atlantic sector of the Southern Ocean, *Earth Planet. Sci. Lett.*, *317*, 282–294.
Stuiver, M., and H. G. Ostlund (1980), GEOSECS Atlantic radiocarbon, *Radiocarbon*, *22*(1), 1–24.
Stuiver, M., P. M. Grootes, and T. F. Braziunas (1995), The GISP2 delta O-18 climate record of the past 16,500 years and the role of the Sun, ocean, and volcanoes, *Quat. Res.*, *44*(3), 341–354.
Svensson, A., et al. (2006), The Greenland Ice Core Chronology 2005, 15–42 ka. Part 2: Comparison to other records, *Quat. Sci. Rev.*, *25*(23–24), 3258–3267.
Tachikawa, K., V. Athias, and C. Jeandel (2003), Neodymium budget in the modern ocean and paleo-oceanographic implications, *J. Geophys. Res.*, *108*(C8), 3254, doi:10.1029/1999JC000285.
Tanaka, T., et al. (2000), JNdi-1: A neodymium isotopic reference in consistency with LaJolla neodymium, *Chem. Geol.*, *168*(3–4), 279–281.
Tessin, A. C., and D. C. Lund (2013), Isotopically depleted carbon in the mid-depth South Atlantic during the last deglaciation, *Paleoceanography*, *28*, 296–306, doi:10.1002/palo.20026.
Thiagarajan, N., D. Gerlach, M. L. Roberts, A. Burke, A. McNichol, W. J. Jenkins, A. V. Subhas, R. E. Thresher, and J. F. Adkins (2013), Movement of deep-sea coral populations on climatic timescales, *Paleoceanography*, *28*, 227–236, doi:10.1002/palo.20023.

Thiagarajan, N., A. V. Subhas, J. R. Southon, J. M. Eiler, and J. F. Adkins (2014), Abrupt pre-Bolling-Allerod warming and circulation changes in the deep ocean, *Nature*, *511*(7507), 75–78.

Thomas, A. L., G. M. Henderson, and L. F. Robinson (2006), Interpretation of the $^{231}Pa/^{230}Th$ paleocirculation proxy: New water-column measurements from the southwest Indian Ocean, *Earth Planet. Sci. Lett.*, *241*(3–4), 493–504.

Thornalley, D. J. R., I. N. McCave, and H. Elderfield (2011a), Tephra in deglacial ocean sediments south of Iceland: Stratigraphy, geochemistry and oceanic reservoir ages, *J. Quat. Sci.*, *26*(2), 190–198.

Thornalley, D. J. R., S. Barker, W. S. Broecker, H. Elderfield, and I. N. McCave (2011b), The deglacial evolution of North Atlantic deep convection, *Science*, *331*(6014), 202–205.

van de Flierdt, T., L. F. Robinson, J. F. Adkins, S. R. Hemming, and S. L. Goldstein (2006), Temporal stability of the neodymium isotope signature of the Holocene to glacial North Atlantic, *Paleoceanography*, *21*, PA4102, doi:10.1029/2006PA001294.

van de Flierdt, T., L. F. Robinson, and J. F. Adkins (2010), Deep-sea coral aragonite as a recorder for the neodymium isotopic composition of seawater, *Geochim. Cosmochim. Acta*, *74*(21), 6014–6032.

Voelker, A. H. L., M. Sarnthein, P. M. Grootes, H. Erlenkeuser, C. Laj, A. Mazaud, M. J. Nadeau, and M. Schleicher (1998), Correlation of marine ^{14}C ages from the Nordic Seas with the GISP2 isotope record: Implications for ^{14}C calibration beyond 25 ka BP, *Radiocarbon*, *40*(1), 517–534.

von Blanckenburg, F. (1999), Perspectives: Paleoceanography—Tracing past ocean circulation?, *Science*, *286*(5446), 1862–1863.

von Blanckenburg, F., and T. F. Nagler (2001), Weathering versus circulation-controlled changes in radiogenic isotope tracer composition of the Labrador Sea and North Atlantic Deep Water, *Paleoceanography*, *16*(4), 424–434, doi:10.1029/2000PA000550.

Waelbroeck, C., J. C. Duplessy, E. Michel, L. Labeyrie, D. Paillard, and J. Duprat (2001), The timing of the last deglaciation in North Atlantic climate records, *Nature*, *412*(6848), 724–727.

Waelbroeck, C., L. Labeyrie, E. Michel, J. C. Duplessy, J. F. McManus, K. Lambeck, E. Balbon, and M. Labracherie (2002), Sea-level and deep water temperature changes derived from benthic foraminifera isotopic records, *Quat. Sci. Rev.*, *21*(1–3), 295–305.

Waelbroeck, C., L. C. Skinner, L. Labeyrie, J. C. Duplessy, E. Michel, N. V. Riveiros, J. M. Gherardi, and F. Dewilde (2011), The timing of deglacial circulation changes in the Atlantic, *Paleoceanography*, *26*, PA3213, doi:10.1029/2010PA002007.

Wasserburg, G. J., S. B. Jacobsen, D. J. Depaolo, M. T. McCulloch, and T. Wen (1981), Precise determination of Sm/Nd ratios, Sm and Nd isotopic abundances in standard solutions, *Geochim. Cosmochim. Acta*, *45*(12), 2311–2323.

Wilson, D. J., A. M. Piotrowski, A. Galy, and J. A. Clegg (2013), Reactivity of neodymium carriers in deep sea sediments: Implications for boundary exchange and paleoceanography, *Geochim. Cosmochim. Acta*, *109*, 197–221.

Yu, J. M., H. Elderfield, and A. M. Piotrowski (2008), Seawater carbonate ion-$\delta^{13}C$ systematics and application to glacial-interglacial North Atlantic ocean circulation, *Earth Planet. Sci. Lett.*, *271*(1–4), 209–220.

Zahn, R., and A. Stuber (2002), Suborbital intermediate water variability inferred from paired benthic foraminiferal Cd/Ca and $\delta^{13}C$ in the tropical West Atlantic and linking with North Atlantic climates, *Earth Planet. Sci. Lett.*, *200*(1–2), 191–205.